December 2013

Performance Evaluation of Multiple Antenna Systems

M-Adib El Effendi
University of Wisconsin-Milwaukee

PERFORMANCE EVALUATION OF MULTIPLE ANTENNA SYSTEMS

by

M-ADIB EL EFFENDI

A Thesis Submitted in

Partial Fulfillment of the

Requirements for the Degree of

Master of Science

in Engineering

at

The University of Wisconsin-Milwaukee

December 2013

ABSTRACT

PERFORMANCE EVALUATION OF MULTIPLE ANTENNA SYSTEMS

by

M-ADIB EL EFFENDI

The University of Wisconsin-Milwaukee, 2013
Under the Supervision of Professor Devendra Misra

Wireless traffic is in a continuous increase and there are growing demands for wireless systems that support higher interference suppression and noise mitigation for mobile and cellular communications. Single antenna systems use frequency or time diversity to overcome the multipath fading effect as it represents a major problem that results in sever performance degradation. However, frequency diversity is inefficient in terms of bandwidth requirements and time diversity needs slow time varying channels. Space diversity has been proposed as an alternative to the former schemes where more antennas are added to the transmitter and/or receiver. Nevertheless, when multiple antennas are used; two different gains can be employed to boost system performance represented by the space diversity gains and array gain and it is not yet clear which gain has better performance as most of the published work study each one separately. Further, there is a variety of beamforming algorithms can achieve a high array gain to mitigate noise and interference. However, because each algorithm uses a different approach to achieve this goal, an ambiguity arises in some of their performance aspects as it is possible that some algorithms may have similar performance in interference suppression but varies in their

capability in mitigating noise or vice versa. This may have a big impact on their performance in some environments where the interference and noise floors vary considerably and yet no study has fully addressed this problem. In this work, multiple input multiple output antenna systems were investigated using a variety of antenna configurations and algorithms to evaluate their performance under different noise and interference levels using MATLAB software modeling tools. It was found that array gain gives higher system performance in comparison with the space diversity gain and can be considered the most optimal scheme. After analyzing the performance of different beamformers, it was found that phase shift and MVDR beamformers both have the same capability in mitigating white noise while they vary in their ability in interference suppression depending on the level of SINR of the surrounding environment. Also, Frost beamformer shows high interference suppression while its noise mitigation capability is very low which limits its use in applications where the noise floor is higher than the interference floor.

Keywords: beamformers, transmit diversity, receive diversity, space time coding

TABLE OF CONTENTS

LIST OF FIGURES

LIST OF ABBREVIATIONS

BC	Broadcast Channel
BS	Base Station
CLMS	Constrained Least Mean Squares
CSI	Channel State Information
DFT	Discrete Fourier Transform
DoA	Direction of Arrival
DPC	Dirty Paper Coding
EF	Element Factor
iid	identically independent distributed
LCMV	Linear Constraint Minimum Variance
LTE	Long Term Evolution
MAC	Multiple Access Channel
MIMO	Multiple Input Multiple Output
ML	Maximum Likelihood
MMSE	Minimum Mean Square Error
MS	Mobile station

MRC	Maximum Ratio Combining
MVDR	Minimum Variance Distortionless Response
OSTBC	Orthogonal Space Time Block Coding
THP	Tomlinson-Harashima Precoding
SISO	Single Input Single Output
SINR	Signal to Interference and Noise Ratio
SNR	Signal to Noise Ratio
SVD	Singular Value Decomposition
TCM	Trellis Coded Modulation
ULA	Uniform Linear Array
ZF	Zero Forcing

Chapter 1: Introduction

1.1 Background and previous work:

Multiple input multiple output (MIMO) antenna systems have been a hot topic for investigation for the last two decades due to their promising capabilities in providing high data rates and better performance in comparison with single input single output (SISO) systems. One of the main problems in wireless systems is the characteristics of the wireless channel which has a big impact on the quality of the overall system due to multipath fading. In general, the behavior of the wireless channel varies depending on the environment that surrounds both the transmitter and receiver sides. For example, in satellite communication systems where there is a direct line of sight between the communicating units; multipath fading is negligible, but in cellular and mobile communications scenarios where there are a lot of obstacles and no direct line of sight is available between the transmitting and receiving units; different replicas of the original signal arrive to the receiver from different paths which can be added either constructively or destructively depending on the phase or time delay of each replica [1] and results in multipath fading. Signal multipath fading is directly affected by the speed of both the transmitting and receiving ends such that fading increases with increasing speed and vice versa. Mitigating this problem can be done by increasing the transmission power of the wireless link in order to increase the signal to noise ratio which results in improved system performance, but this technique is power consuming especially for handheld mobile devices in which battery life time is extremely important. Other techniques use time or frequency diversity to solve this problem. However, time diversity suffers from

large delays in slow varying channels because it uses time interleaving [2]. On the other hand frequency diversity consumes high bandwidth which is a big waste of the frequency spectrum. A previous work conducted in 1991 by Wittneben [3, 4] suggested the use of space diversity to improve performance and his method is based on using finite impulse response filters with different coefficients that are chosen to achieve optimal diversity gain. In 1997 Seshadri and Tarokh [5] made a big contribution by designing space time trellis codes for multiple antenna systems, and it combines transmit diversity with forward error correction to achieve high performance gains. However, their design comes with a big cost of more processing which increases as a function of both the diversity order and bandwidth efficiency [2]. To fully address this problem, Alamouti [2] proposed in 1998 a novel scheme that uses two transmit antennas and one receive antenna using special space time block codes that are simple to implement and can achieve an improved performance while maintaining a constant bandwidth. A lot of contributions have been made since then and in the same year Tarokh [6] proposed a novel technique that adds a coding gain which results in better performance. Before that time, space diversity was achieved by increasing the number of antennas at the receiver side while employing one antenna at the transmitter side and the diversity which results from this method is called receive diversity. However, this method has a big disadvantage represented by the more computational complexity at the receiver side. However, the techniques that are adopted to achieve transmit diversity are different from those used to achieve receive diversity. In the first case the proposed space time coding by Alamouti is used while in the second situation maximum ratio combining is employed at the receiving unit. It should be mentioned that transmit diversity can be achieved even if two or more

antennas are used in the receiver as long as space time encoder and decoder are used in the transmitter and receiver chains respectively. Nevertheless, as long as encoding in the transmitter side manifests itself in more processing times, the corresponding system may show a slow behavior and supply low data rates. Other schemes have been proposed to replace the encoding and decoding chains with linear signal detection methods at the receiver side to get higher data rates but there is an ambiguity in terms of their level of performance compared with the transmit and receive diversity schemes. All the former methods are for single user MIMO systems where one user exists in the network. In multiuser MIMO systems, the situation becomes more complicated as another problem represented by interference coming from different users is added to the multipath fading problem. Therefore, other techniques are needed to deal with this situation because the aforementioned schemes do not have the capability of interference suppression. Since 2001 a lot of researchers contributed to overcome this obstacle starting from Caire and Shamai [7] who proposed in that year a precoding method called dirty paper coding (DPC) to overcome the overall channel effect and showed an acceptable performance. In 2002 Fischer and others [8] applied Tomlinson-Harashima Precoding invented by Harashima in 1972 which uses a precoding technique to eliminate interference and has low power requirements. The final contribution came by Peel and others [9] in 2005 when they proposed a technique that improves performance by regularizing the inverse of the channel response through the addition of an identity matrix. All of these three techniques assume one antenna is present at the receiver side represented by the mobile unit where no space diversity is available to the receiver. However, if the receiving unit has two or more antennas then space diversity can be used to suppress multipath fading

while the interference problem still exists. This problem has been a predicament until finally cracked in 2004 by Choi and Murch [10] who were able to decompose the multiuser MIMO channel to single user MIMO channels which cancel all interference and then linear detection techniques can be used at the receiver to suppress the multipath fading problem. All of the presented schemes employ omnidirectional antennas where no beam directivity exists. On the other hand, there is a lack of investigation that study the application beamformers used for radar and sonar in mobile communications where directional beams are formed to the desired users and array gains are achieved instead of diversity gains. For this purpose, there are a lot of statistical algorithms can be applied to optimize system performance on the receiver side such as Frost [11], Minimum Variance Distortionless Response (MVDR) and Least Constrained Minimum Variance (LCMV) algorithms [12] based on minimizing the mean squared error, while the phase shift approach [13] can be employed at both at the receiver and transmitter sides. The phase shift approach improves performance at the receiver by making an alignment of the received signal phases to achieve constructive addition of waveforms, while it adjusts the phases of the antenna elements at the transmitter to form directional beams to the intended receiver. However, the performance of each algorithm among others is totally unclear. Further, a clear judgment weather beamforming outperforms space diversity techniques remains missing.

1.2 Problem description and thesis overview:

Although there have been a lot of investigations that studied multiple antenna systems for both single user and multiuser scenarios, a lot of gaps in each scenario still exist because those investigations are recent. In the single user systems, a fair comparison that

addresses the performance of space diversity under the same conditions is still missing. Further, most of the investigations that treated multiuser systems do not take into account the increased number of users on system performance and as the performance depends on the number of antennas in the receiving unit, they do not show a complete performance comparison between single antenna and multiple antenna receivers under similar conditions as well. This work tries to bridge these gaps to offer a fair comparison between the single user MIMO systems on one hand and multiuser MIMO systems on the other hand to find the optimal scheme for each case. The major contribution of this work is to study the performance of beamforming systems represented by phase shift, MVDR, LCMV and Frost beamformers, and give a detailed analysis of their capabilities in suppressing interference and noise under different interference and noise floors to fully address the usability of each beamformer in different applications. This is because most of the published studies do not take into account the level of noise and interference floors separately on the overall ability of beamformers in achieving sufficient performance in applications where the noise and interference floors vary significantly. Therefore, a detailed analysis is required that takes those points into account which is the basic aim of this work. A further step is taken to model some of the performance aspects with mathematical functions using OriginLab analysis software to enable performance predictions in real time applications. Also, a performance comparison between the space diversity schemes and beamforming schemes is presented to find the optimum approach that gives the highest performance possible and consequently make a judgment weather beamforming outperforms space diversity techniques.

Chapter 2: Single User MIMO Systems

Chapter Summary:

In this chapter, the aim is to resolve part of the ambiguity that governs some of the performance aspects of the space diversity schemes for single user MIMO systems. In this work, the outdoor fading environment is considered where multipath fading exists. First, the basic principles and theory that describe the single user schemes are presented then the results and findings of this work are listed.

2.1) Introduction:

Modern wireless communication systems and mobile technology use smart antenna systems that have capabilities in adapting with different conditions of the wireless channel in order to support both high quality and data rates for mobile users. The ability of smart phones that employ this type of antennas to cope with the changes of the indoor and outdoor environments requires adaptive techniques to make radio communications more robust. Traditional systems use time and frequency diversity techniques which are based on the principle that says: the probability that multiple statistically independent fading channels experience deep fading simultaneously is very low [14]. Based on this idea the former diversity techniques work as follows:

1) Time diversity:

In this technique the signal of interest is transmitted over different time slots, and because the channel conditions change with time; there should be one time instance where at least one of the transmitted versions of the signal experience low fading [15].

2) Frequency diversity:

This scheme transmits the signal of interest on different frequencies with a frequency separation big enough to make the fading that occurs at one frequency different from the fading which occurs at the other frequency [16]. However, because the frequency spectrum is a scarce resource this makes such type of scheme inefficient [16].

3) Space diversity:

MIMO antenna systems use a diversity scheme that is different from the former two schemes called space diversity which uses multiple antennas that are sufficiently separated in order to make the signal in each path experience a different fading such that the correlation between paths is very small [17]. This scheme can be divided into transmit diversity, receive diversity [17] and spatial multiplexing techniques. Figure 2.1 shows the former diversity schemes:

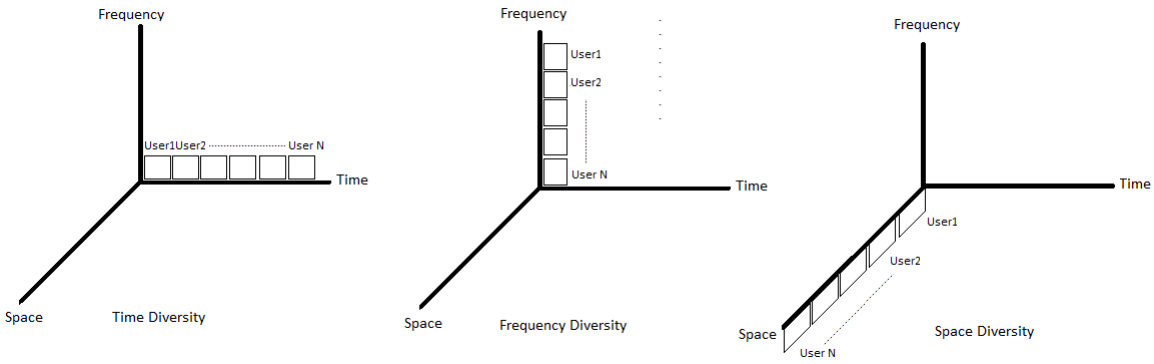

Figure 2.1 Illustrations of time, frequency, and space diversity techniques

2.2) MIMO channel model:

In order to study the performance of MIMO systems, it is important to understand the behavior of MIMO channels because it is different from the channel model that

characterizes the behavior of the general wireless single input single output (SISO) system. The models that describe the indoor and outdoor environments are different and in this work the outdoor case is considered where a Base Station (BS) and a Mobile Station (MS) exchange wireless data as shown in Fig. 2.2:

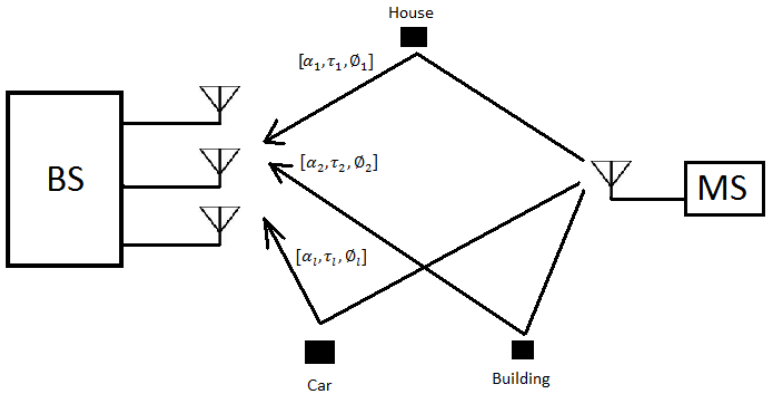

Figure. 2.2 MIMO wireless channel model

One of most recent models that provide an accurate description of the above channel was developed by Pedersen and others [18] in the year of 2000 using a simple statistical model. In this model, assuming a Uniform Linear Antenna (ULA) array; the received baseband signal vector can be written as (bold style letters refer to a matrix notation through this work) [18]:

$$\boldsymbol{Y}(t) = \sum_{l=1}^{L} \alpha_l \boldsymbol{C}(\emptyset_l) u(t-\tau_l) + \boldsymbol{N}(t) \ldots\ldots\ldots (1.1)$$

α_l: the complex amplitude of the l_{th} component.

τ_l: delay of the l_{th} component.

$\emptyset_l$: incidence azimuth of the l_{th} component.

$u(t)$: transmitted information signal

Here it has been assumed that $[\alpha_1, \tau_1, \emptyset_1], [\alpha_2, \tau_2, \emptyset_2]$ … … … … $[\alpha_l, \tau_l, \emptyset_l]$ are independent identically distributed (iid) processes. The received signal vector can be written as [18]:

$$\boldsymbol{Y}(t) = [Y_1(t), Y_2(t), Y_3(t), \ldots \ldots Y_M(t)]^T \ldots\ldots (1.2)$$

Where the components in $\boldsymbol{Y}(t)$ are the signals at the output of the M antenna elements. $\boldsymbol{C}(\emptyset_l)$ is the array steering vector and can be omitted in space diversity schemes where no directional beams are formed and it can be written as [18]:

$$\boldsymbol{C}(t) = [C_1(\emptyset), C_2(\emptyset), C_3(\emptyset), \ldots \ldots C_M(\emptyset)]^T \ldots\ldots (1.3)$$

$\boldsymbol{N}(t)$ is a complex white Gaussian noise processes with identical power density [18]:

$$\boldsymbol{N}(t) = [N_1(t), N_2(t), N_3(t), \ldots \ldots N_M(t)]^T \ldots\ldots (1.4)$$

2.3) Transmit Diversity:

The general block diagram of the transmit diversity scheme is shown in Fig. 2.3 below:

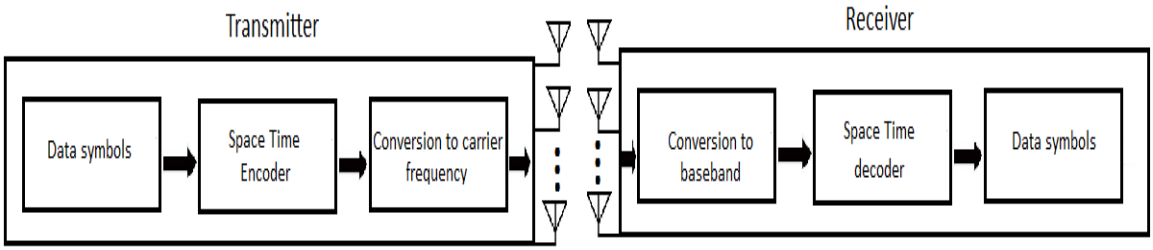

Figure 2.3 General block diagram of transmit diversity MIMO systems

2.3.1) Alamouti Scheme:

Transmit diversity is used in the uplink where MSs transmit data streams to the BS. As mentioned before, Alamouti was the first who invented this approach and here the basic

principles of this scheme are shown. Figure 2.4 clarifies Alamouti's approach which is a specific case of the former block diagram:

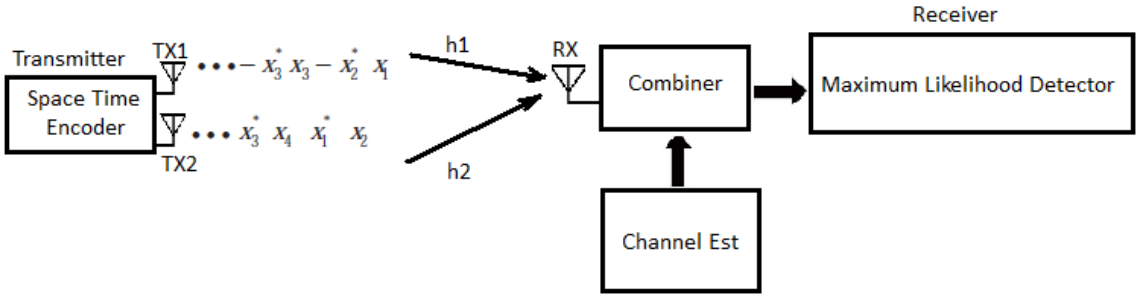

Figure 2.4 Alamouti Scheme

The basic idea of this scheme is to achieve the diversity gain which is defined as the increase in the signal to noise ratio in a MIMO antenna system compared to the gain of a SISO antenna system [19]. This is done by transmitting two replicas of each symbol through each of the transmitting antennas in two different time slots in order to make the fading of the replicas independent of each other [20], and here the process details are shown. Assuming two channel gains $h_1(t)$ and $h_2(t)$ along a time invariant channel [14]:

$$h_1(t) = h_1(t + T_s) = h_1 = |h_1|e^{-j\alpha_1} \ldots\ldots\ldots (1.5)$$

$$h_2(t) = h_2(t + T_s) = h_2 = |h_2|e^{-j\alpha_2} \ldots\ldots\ldots (1.6)$$

Where $|h|$and α denote the amplitude gain and phase rotation respectively. In the first time slot, the information symbols $X_1$and X_2 are transmitted by the antennas Tx1 and Tx2 respectively, and the received signal $y_1$at the end of the first time slot is [20]:

$$y_1 = h_1X_1 + h_2X_2 + n_1 \ldots\ldots\ldots (1.7)$$

Where n_1 is a complex noise sample. During the second time slot, a transformed version of the two symbols is transmitted such that the negative conjugate of X_2 is transmitted by Tx1 and the conjugate of X_1 is transmitted by Tx2 as shown in Fig. 2.4 above. In other words, the assignment of the time slots to the transmitter antennas is swapped, therefore; the received signal at the end of the second time slot can be expressed as [20]:

$$y_2 = -h_1 X_2^{*} + h_2 X_1^{*} + n_2 \ldots\ldots\ldots (1.8)$$

Where n_2 is a complex noise sample. The idea behind the transform and swap is that the consecutive time slots are not faded independently, therefore; no diversity gain would be achieved by mapping the transformed replicas to the same antennas of the first time slot [20]. At the receiver side, the two transmitted symbols are separated using a channel estimator as shown in Fig. 2.4. Therefore; the extracted symbols are [20]:

$$\tilde{X}_1 = \overline{h_1} y_1 + h_2 \overline{y_2} = (|h_1|^2 + |h_2|^2) X_1 + \overline{h_1} n_1 + h_2 \overline{n_2} \ldots\ldots\ldots (1.9)$$

$$\tilde{X}_2 = \overline{h_2} y_1 - h_1 \overline{y_2} = (|h_1|^2 + |h_2|^2) X_2 + \overline{h_2} n_1 - h_1 \overline{n_2} \ldots\ldots\ldots (1.10)$$

Alamouti code word can be expressed in a matrix form as [14]:

$$\boldsymbol{X} = \begin{bmatrix} X_1 & -X_2^{*} \\ X_2 & X_1^{*} \end{bmatrix} \ldots\ldots\ldots (1.11)$$

By using a maximum likelihood detector; the receiver can decide the more likely transmitted symbol based on the lowest Euclidean distance measure [20]. One of the important properties of this codeword is orthogonality and all codes that use the above principle are called orthogonal space time block codes (OSTBC), and this can be shown as follows where **I** is the identity matrix [14]:

$$\boldsymbol{X}.\boldsymbol{X^H} = \begin{bmatrix} |X_1|^2 + |X_2|^2 & 0 \\ 0 & |X_1|^2 + |X_2|^2 \end{bmatrix} = (|X_1|^2 + |X_2|^2)\boldsymbol{I} \Rightarrow \boldsymbol{X} \text{ is orthogonal}$$

2.3.2) Generalization on Alamouti Scheme:

Alamouti scheme can be expanded to engage N_T transmit antennas and N_R receive antennas as shown in Fig. 2.5:

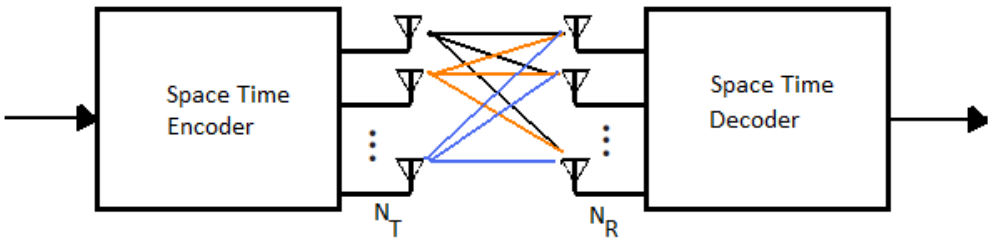

Figure 2.5 Alamouti scheme for $N_T X N_R$ system

If ${X_i}^{(t)}$is the transmitted signal from the i_{th}transmit antenna during t_{th}symbol period, the received signal at the j_{th}receive antenna during the t_{th}symbol period can be given as [14]:

$$y_j{}^{(t)} = \sqrt{\frac{E_x}{N_0 N_T}} \left[h_{j1}{}^{(t)} \; h_{j2}{}^{(t)} \ldots\ldots h_{jN_T}{}^{(t)}\right] \begin{bmatrix} X_1{}^{(t)} \\ \cdot \\ \cdot \\ \cdot \\ X_{N_T}{}^{(t)} \end{bmatrix} + Z_j{}^{(t)} \ldots\ldots (1.12)$$

Where N_0 and E_x are the noise and signal powers respectively. During a period of T symbols for the j_{th}receive antenna, the former relation becomes [14]:

$$\left[y_1{}^{(t)} \; y_2{}^{(t)} .. y_j{}^{(t)}\right] = \sqrt{\frac{E_x}{N_0 N_T}} \left[h_{j1}{}^{(t)} \; h_{j2}{}^{(t)} \ldots\ldots h_{jN_T}{}^{(t)}\right] \begin{bmatrix} X_1{}^{(1)} & X_1{}^{(1)} & & X_1{}^{(T)} \\ \cdot & \cdot & & \cdot \\ \cdot & \cdot & \ldots & \cdot \\ \cdot & \cdot & & \cdot \\ X_{N_T}{}^{(1)} & X_{N_T}{}^{(2)} & & X_{N_T}{}^{(T)} \end{bmatrix}$$

$$+\left[Z_j{}^{(1)} Z_j{}^{(2)} \ldots Z_j{}^{(T)}\right] \ldots\ldots (1.13)$$

If N_R receive antennas are assumed then it is possible to write [14]:

$$\begin{bmatrix} y_1^{(1)} & y_1^{(2)} & & y_1^{(T)} \\ \vdots & \vdots & \dots & \vdots \\ y_{N_R}^{(1)} & y_{N_R}^{(2)} & & y_{N_R}^{(T)} \end{bmatrix} = \sqrt{\frac{E_x}{N_0 N_T}} \begin{bmatrix} h_{11}^{(1)} & h_{12}^{(1)} & & h_{1N_T}^{(T)} \\ \vdots & \vdots & \dots & \vdots \\ h_{N_R1}^{(1)} & h_{N_R2}^{(2)} & & h_{N_R N_T}^{(T)} \end{bmatrix}$$

$$x \begin{bmatrix} X_1^{(1)} & X_1^{(1)} & & X_1^{(T)} \\ \vdots & \vdots & \dots & \vdots \\ X_{N_T}^{(1)} & X_{N_T}^{(2)} & & X_{N_T}^{(T)} \end{bmatrix} + \begin{bmatrix} z_1^{(1)} & z_1^{(2)} & & z_1^{(T)} \\ \vdots & \vdots & \dots & \vdots \\ z_{N_R}^{(1)} & z_{N_R}^{(2)} & & z_{N_R}^{(T)} \end{bmatrix} \dots\dots (1.14)$$

2.3.3) Transmit Diversity with Channel State Information (CSI):

In the above approach only the receiver knows the channel state information (CSI). However, if the transmitter can get a feedback about CSI then the diversity gain should be improved. This can be done through the use of codewords which leads to the principle of precoding. In this approach the CSI is represented by codewords in a form of quantized vectors [14]. The receiver at the receiving end estimates the CSI and maps this information to the most appropriate codeword and feeds the index of the corresponding codeword back to the transmitter which already has the same codeword list. The transmitter then gets a sense of the CSI and adjusts the transmitted signal by picking another codeword that reverses the effect of the channel [14]. Figure 2.6 shows this scheme:

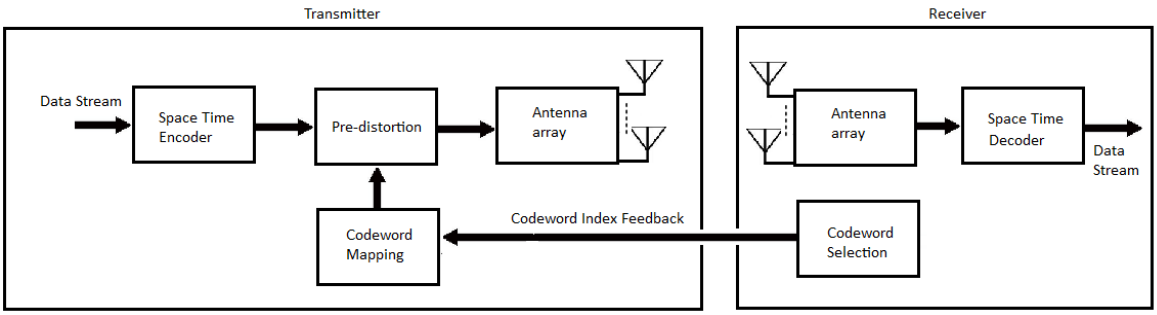

Figure 2.6 Block diagram of transmit diversity with precoding

The question here is how to design the codewords in order to achieve improved system performance. Love and Heath [21] answered this question in a paper published in 2005 when they suggested a codeword design criterion that minimizes the error probability of the symbol errors of the precoded system. Consequently, the transmitted symbol is multiplied by a codeword in advance that opposes the channel response and the received signal is given as [14]:

$$\boldsymbol{y} = \sqrt{\frac{E_x}{N_T}}\boldsymbol{hWC} + \boldsymbol{z} \ldots\ldots (1.15)$$

Where **h** is the channel matrix vector, **W** is the precoding matrix vector, **Z** is the noise vector, **C** is the codeword matrix vector, N_T is the noise power and E_x is the signal power. The error probability can be expressed as [14]:

$$\Pr(Error|\boldsymbol{H}) \leq \exp\left(-\frac{E_x}{N_0}\frac{||\boldsymbol{HWE}_{i,j}||^2}{4N_T}\right) \ldots\ldots (1.16)$$

Where $||.||^2$is a second order norm and $E_{i,j} = C_i - C_j$ is the error matrix between the transmitted and received codewords C_i and C_j $(i \neq j)$. According to Love and Heath, the

optimum codeword W_{opt} will be the one that minimizes this error probability function which consequently maximizes $\boldsymbol{HWE}_{i,j}$ [14]:

$$W_{opt} = \arg Max_{\boldsymbol{W}\in F, i\neq j} ||\boldsymbol{HWE}_{i,j}||^2{}_F = \arg Max_{\boldsymbol{W}\in F} ||\boldsymbol{HW}||^2{}_F \ldots\ldots (1.17)$$

Where *F* is a codebook which contains a set of codewords such that [14]:

$$F = \{\boldsymbol{W_1}, \boldsymbol{W_2}, \ldots\ldots, \boldsymbol{W_M}\} \ldots\ldots (1.18)$$

The design of the former codewords is beyond the scope of this research. However, here the practical codewords that are adopted by the IEEE 802.16e specification are used in this work and were proposed by a team of researchers in Bell Labs and based on Discrete Fourier Transform (DFT) [22]:

$$F = \{\boldsymbol{W_{DFT}}, \boldsymbol{\theta W_{DFT}}, \ldots\ldots, \boldsymbol{\theta^{L-1} W_{DFT}}\} \ldots\ldots (1.19)$$

The proposed coefficient is given as [22]:

$$\boldsymbol{W}_{DFT} = \frac{1}{\sqrt{T}} \begin{bmatrix} 1 \\ e^{i\frac{2\pi}{L}(l-1)} \\ e^{i\frac{2\pi}{L}2(l-1)} \\ \cdot \\ \cdot \\ e^{i\frac{2\pi}{L}(T-1)(l-1)} \end{bmatrix}; \quad T, l = 1,2, \ldots\ldots, N_T. \quad \ldots\ldots (1.20)$$

Where L is the number of points in Fourier Transform, and θ is [22]:

$$\boldsymbol{\theta} = \begin{bmatrix} e^{i\frac{2\pi}{L}u_1} & \cdots & 0 \\ \vdots & \ddots & \vdots \\ 0 & \cdots & e^{i\frac{2\pi}{L}u_T} \end{bmatrix} = diag\left(\left[e^{i\frac{2\pi u_1}{N_T}} \; e^{i\frac{2\pi\, u_2}{N_T}} \; e^{i\frac{2\pi\, u_3}{N_T}} \ldots\ldots e^{i\frac{2\pi\, N_T}{N_T}}\right]\right) \ldots\ldots (1.21)$$

The u_i variables are determined such that the following minimum chordal distance is maximized [14]:

$$\boldsymbol{u} = \arg max_{\{u_1,u_1,\ldots u_{N_T}\}} \min_{l=1,2,\ldots N_T-1} d(\boldsymbol{W_{DFT}}, \boldsymbol{\theta^l W_{DFT}}) \ldots\ldots (1.22)$$

In the case of IEEE 802.16e WiMax the above variables are given as [14]:

$$W_1 = \frac{1}{\sqrt{4}} \begin{bmatrix} 1 & 1 & 1 \\ 1 & e^{i\frac{2\pi\,2}{4}} & e^{i\frac{2\pi\,3}{4}} \\ 1 & e^{i\frac{2\pi\,4}{4}} & e^{i\frac{2\pi\,6}{4}} \\ 1 & e^{i\frac{2\pi\,6}{4}} & e^{i\frac{2\pi\,9}{4}} \end{bmatrix},$$

$$W_i = diag\left(e^{i\frac{2\pi}{4}}\ e^{i\frac{2\pi\,8}{4}}\ e^{i\frac{2\pi\,61}{4}}\ e^{i\frac{2\pi\,45}{4}}\right)^{i-1} W_1, i = 2,..64. \quad \ldots\ldots (1.23)$$

2.4) Receive Diversity:

Another method for achieving high performance is to use more antennas at the receiver side with maximum ratio combining (MRC) to get a receive diversity while one antenna is used at the transmitter. In this case, the space time block coding is not used as in the transmit diversity scheme, but the noise effect is alleviated by the use of MRC at the receiver. The MRC scheme works by combining the signals with the highest magnitude while the rest of the received signals are attenuated as shown in Fig. 2.7:

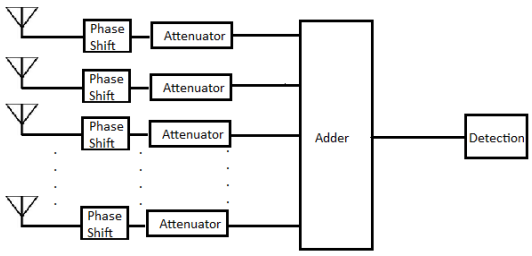

Figure 2.7 MRC scheme

The combined signal can be expressed as [14]:

$$y_{MRC} = \sqrt{\frac{E_X}{N_0}}\boldsymbol{Whx} + \boldsymbol{Wz} \ldots\ldots (1.24)$$

WhereE_X, N_0 are the signal and noise powers respectively, x is the received signal, $\boldsymbol{h}$ represents the channel response matrix and $\boldsymbol{z}$ is a noise vector. $\boldsymbol{W}$ is a weight vector that represents a phase shift to make appropriate alignment of the received signal phases and it is found such that the signal to noise ratio is maximized [14]:

$$\rho = \frac{E_X}{N_0}\frac{|\boldsymbol{Wh}|^2}{||\boldsymbol{W}||^2} \ldots\ldots (1.25)$$

The above ratio is maximized at $\boldsymbol{W} = \boldsymbol{h}^*$which yields $\rho = \frac{E_X}{N_0}||h||^2$[14].

2.5) Spatial Multiplexing:

Other methods of implementation depend totally on signal detection algorithms of the spatially multiplexed signals at the receiver side without any coding or additional processing at the transmitter. Here three methods for linear detection are presented.

2.5.1) Linear Detection:

Linear detection aims to cancel all signals except the signal of interest from the desired antenna [14]. There are three basic methods that can be used to detect spatially multiplexed signals; zero forcing (ZF) detection, minimum mean square error (MMSE) detection and maximum likelihood (ML) detection. The ZF and MMSE methods decouple the received MIMO signals into uncorrelated signals [23] and the detection of

each symbol is given by a linear combination of the received signals [14]. Figure 2.8 shows a general block diagram of spatially multiplexed MIMO systems:

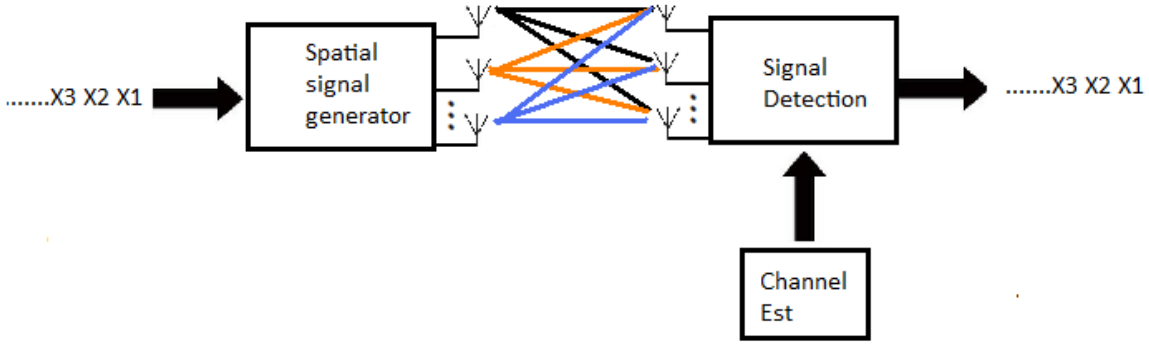

Figure 2.8 Spatially multiplexed MIMO systems

2.5.1.1) ZF Detection:

The ZF technique cancels the channel effect by using the following matrix [14]:

$$\boldsymbol{W_{ZF}} = (\boldsymbol{H}^H\boldsymbol{H})^{-1}\boldsymbol{H}^H \ldots\ldots (1.26)$$

The detected symbol is found as [14]:

$$\widetilde{\boldsymbol{X}}_{\boldsymbol{ZF}} = \boldsymbol{W_{ZF}Y} = \boldsymbol{X} + (\boldsymbol{H}^H\boldsymbol{H})^{-1}\boldsymbol{H}^H\boldsymbol{Z} = \boldsymbol{X} + \widetilde{\boldsymbol{Z}}_{\boldsymbol{ZF}} \ldots\ldots (1.27)$$

Where $(.)^H$is the Hermitian transpose operation. The power of the expected value of the noise is found to be [14]:

$$E\{||\widetilde{\boldsymbol{Z}}_{\boldsymbol{ZF}}||^2\} = \sum_{i=1}^{N_T} \frac{\boldsymbol{\sigma_z}^2}{\boldsymbol{\sigma_i}^2} \ldots\ldots (1.28)$$

Where $\boldsymbol{\sigma_z}$and $\boldsymbol{\sigma_i}$ are the variances of noise and signal respectively.

2.5.1.2) MMSE Detection:

The MMSE algorithm detects the transmitted symbol by minimizing the mean squared error $\{(\widetilde{\boldsymbol{X}} - \boldsymbol{X})(\widetilde{\boldsymbol{X}} - \boldsymbol{X})^H\}$ [23], and the weight matrix is given as [14]:

$$\boldsymbol{W}_{\mathbf{MMSE}} = (\boldsymbol{H}^H\boldsymbol{H} + \boldsymbol{\sigma_z}^2\boldsymbol{I})^{-1}\boldsymbol{H}^H \ldots\ldots (1.29)$$

Where $\boldsymbol{\sigma_z}$ is the noise variance that needs to be known at the receiver. The i_{th} row vector $\boldsymbol{w}_{\mathbf{i,MMSE}}$ can be found by optimizing [14]:

$$\boldsymbol{w}_{\mathbf{i,MMSE}} = \mathbf{arg}_{\boldsymbol{w}=(w_1,w_2,\ldots\ldots,w_{N_T})}\ \mathbf{max}\frac{|\boldsymbol{wh_i}|^2 E_X}{E_X\sum_{j=1,j\neq i}^{N_T}|\boldsymbol{wh_i}|^2 + ||\boldsymbol{w}||^2\,\boldsymbol{\sigma_z}^2} \ldots\ldots (1.30)$$

The estimated symbol at the receiver is [14]:

$$\widetilde{\boldsymbol{X}}_{\mathbf{MMSE}} = \boldsymbol{W}_{\mathbf{MMSE}}\boldsymbol{Y} = (\boldsymbol{H}^H\boldsymbol{H} + \boldsymbol{\sigma_z}^2\boldsymbol{I})^{-1}\boldsymbol{H}^H.\boldsymbol{Y} = \widetilde{\boldsymbol{X}} + (\boldsymbol{H}^H\boldsymbol{H} + \boldsymbol{\sigma_z}^2\boldsymbol{I})^{-1}\boldsymbol{H}^H\boldsymbol{Z}$$

$$= \widetilde{\boldsymbol{X}} + \widetilde{\boldsymbol{Z}} \ldots\ldots (1.31)$$

The expected noise power can be found as [14]:

$$E\left\{||\widetilde{\boldsymbol{Z}}_{\mathbf{MMSE}}||^2\right\} = \sum_{i=1}^{N_T}\frac{\boldsymbol{\sigma_z}^2\boldsymbol{\sigma_i}^2}{(\boldsymbol{\sigma_i}^2 + \boldsymbol{\sigma_z}^2)^2} \ldots\ldots (1.32)$$

2.5.1.3) ML Detection:

The maximum likelihood detection has a very simple principle which is based on the exhaustive search by calculating the Euclidean distance between the received signals and all possible transmitted signal vectors in order to maximize the likelihood function which is shown in Fig 2.9 and given as [24]:

$$P(\boldsymbol{Y}|\boldsymbol{X}) = \frac{1}{(\pi\sigma^2)^N} \exp\left(-\frac{||\boldsymbol{Y}-\boldsymbol{HX}||^2}{\sigma^2}\right) \ldots\ldots (1.33)$$

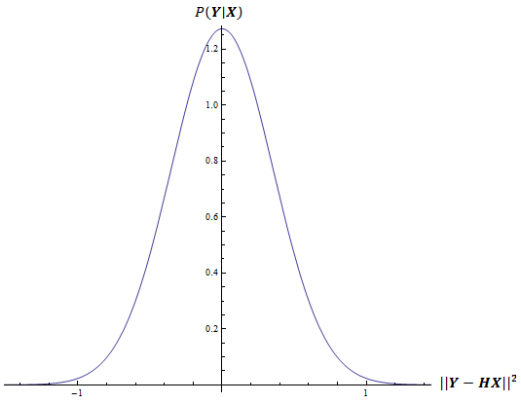

Figure 2.9 Likelihood function

Where: N is the number of all possible vectors. Therefore, the estimated symbol is the one that satisfies the following criteria [14]:

$$\widetilde{\boldsymbol{X}}_{ML} = \arg\min ||\boldsymbol{Y}-\boldsymbol{HX}||^2 \ldots\ldots (1.34)$$

2.6) Results and findings:

Transmit Diversity Versus Receive Diversity:

In this section one of the aims of this work has been met where a detailed comparison between the former single user MIMO schemes is presented under similar conditions to find the optimum scheme which results in the highest performance possible. All analysis assumes outdoor environment and similar noise and multipath fading conditions where a lot of scatterers exist between the transmitting and receiving units. It also assumes single user scenarios with omnidirectional antennas in a flat fading channel environment and both the transmitting and receiving units are not moving. First, the performance of transmit diversity is investigated for different number of transmit antennas and the results

are shown in Fig. 2.10 below (equations 1.5-1.14). It can be seen that increasing the number of antennas at the transmitter increases system performance because the diversity gain increases as well. For example, in the 2X1 system the diversity order is 2 because there are two different paths followed by the signal, and when the diversity order is doubled in the 4X1 system the bit error rate took a further shift downwards indicating better performance. It should be mentioned that OSTBC is a generalization of Alamouti's 2X1 system where the same principle of Alamouti's space time block coding is used.

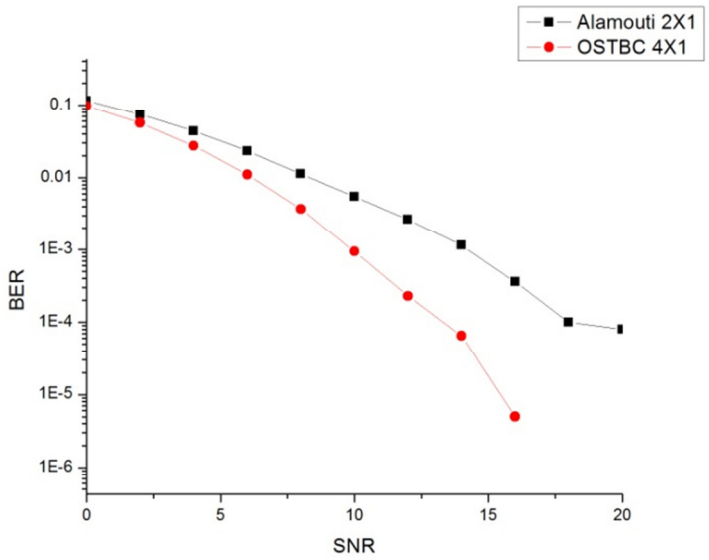

Figure 2.10 Alamouti 2X1and OSTBC 4X1

Next, the same diversity order is maintained but instead of employing 4 antennas at the transmitter; 2 antennas are moved to the receiver and 2 are kept at the transmitter to get 2X2 system. Then, a combiner is implemented at the receiver with ML detection (equation 1.34) in order to combine the received signals from the two antennas, and the results are shown in Fig. 2.11:

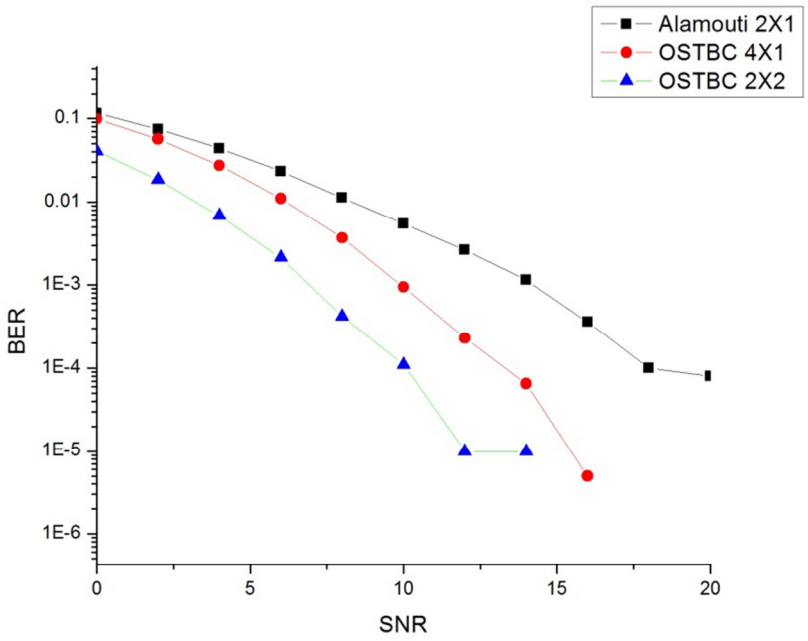

Figure 2.11 OSTBC 4*X*1 compared to 2*X*2

The performance has been improved by a considerable amount although the diversity order did not change and this is because there is a receive diversity gain added to the transmit diversity gain which results in better noise mitigation. Consequently, in order to give a fair judgment weather receive diversity outperforms transmit diversity two systems have been implemented, the first system has 4 transmit antennas and 2 receive antennas (4*X*2 system), and the other has 2 transmit antennas and 4 receive antennas (2*X*4) system (equation 1.14). Both systems have similar fading conditions and employ ML detection at the receiver side (equation 1.34). The results are listed in Fig. 2.12 below:

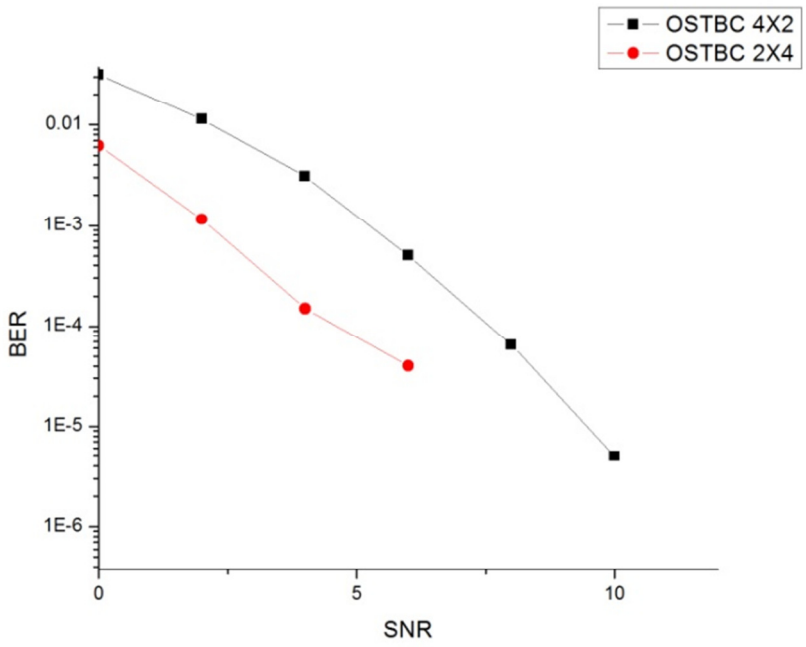

Figure 2.12 4*X*2 Vs 2*X*4 Systems

It is clear that the system which employed 4 antennas at the transmitter has lower performance which reveals that under similar conditions receive diversity outperforms transmit diversity. However, because more antennas at the receiver side implies more processing is required, consequently; if the receiver is a mobile unit then this means shorter battery lifetime because more computations are required to extract the information signal. Next, the precoding scheme employed by IEEE 802.16e WiMax networks is implemented for the sake of finding its noise mitigation capability in comparison with the former schemes. First, percoding has been implemented for 2*X*1 system (equations 1.17- 1.23) and compared with 4*X*1 system without precoding and the results are shown in Fig. 2.13:

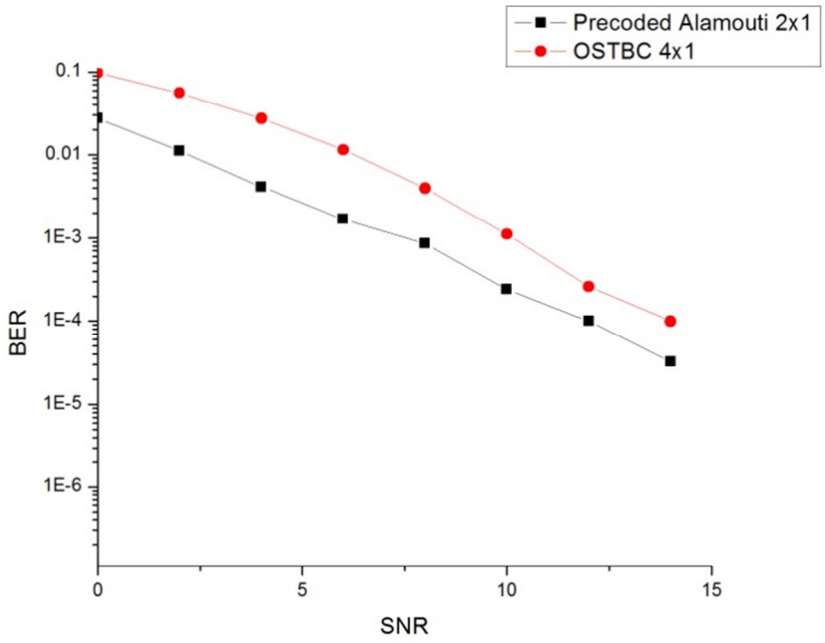

Figure 2.13 OSTBC 4*X*1 Vs Precoded Alamouti 2*X*1

The reported results are highly important because it shows that the 2*X*1 system can achieve better performance with precoding than the 4*X*1 system with no precoding. Therefore, two antennas can be saved which corresponds to saving 50% of the emitted power and consequently reducing 50% of the interference levels taking into account the used antennas are omnidirectional. However, if the percoded 2*X*1 system (equations 1.15-1.23) is compared to the 2*X*2 (equation 1.14) with no precoding (has the same diversity order of 4X1) where both transmit and receive diversity exist, then almost similar performance is observed except at high SNR where the precoded 2X1 seems to have better performance as shown in Fig. 2.14 below:

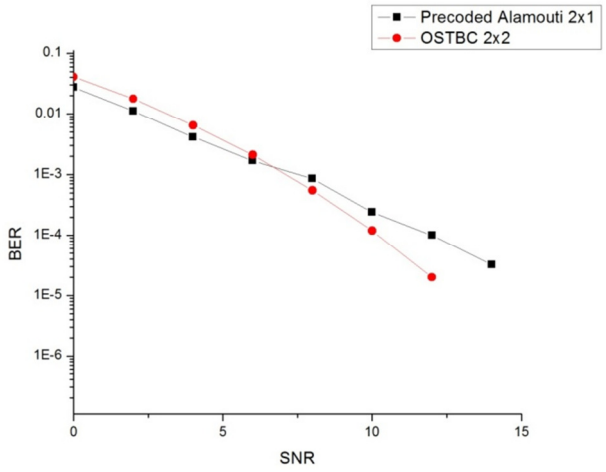

Figure 2.14 Precoded Alamouti 2*X*1 Vs OSTBC 2*X*2

Moving to the receive diversity, transmitter and receiver chains have been implemented in order to address the performance of receive diversity. It is assumed that the receiver has perfect knowledge of the channel state information and the received signal is combined at the receiver using MRC followed by a maximum likelihood detector. First, 1*X*2 system is implemented (equations 1.24, 1.25), then more antennas are added to the receiver and the results are shown in Fig. 2.15 below:

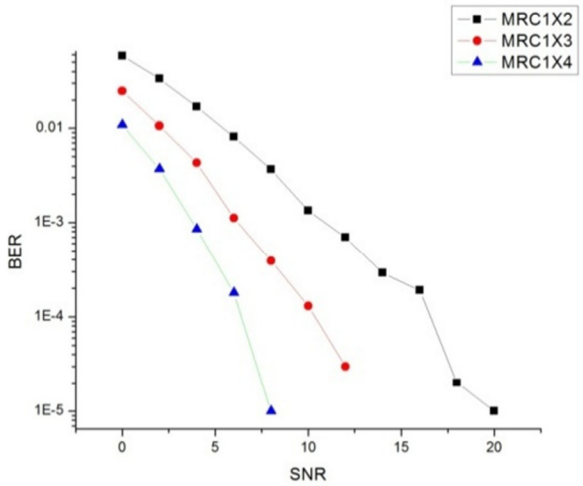

Figure 2.15 System performance of MRC

Increasing the number of antennas at the receiver side improved performance and no space time coding is used in this scheme. Next, precoded Alamuoti 2*X*1 is implemented (equations 1.15-1.23) taken into account the same noise level and channel conditions of the receive diversity scheme (equation 1.34) and the performance of both systems is listed for the sake of comparison as shown in Fig. 2.16:

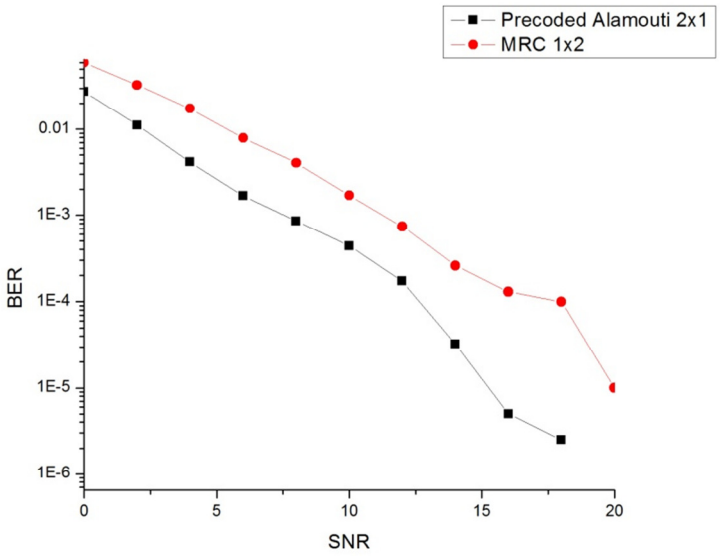

Figure 2.16 MRC 1*X*2 Vs Precoded Alamouti 2*X*1

The reported result is very interesting as it shows that precoded Alamouti which is a transmit diversity scheme where the transmitter has perfect knowledge of the channel state information outperforms the receiver diversity scheme for the same diversity order (which is 2 in this case). This can be explained as follows; noise is added to the signal after being broadcast in the way to the receiver and even if the receiver has perfect knowledge of the channel state information in the receive diversity scheme, there is no possibility to eliminate the effect of noise as it is already combined with the received signal. Therefore, what the receiver does to reduce the noise is combining different

replicas that experience low noise and fading to maximize the signal to noise ratio which has limited capability as the receiver cannot control the amount of added noise in the signal. On the other hand, if the transmitter has perfect knowledge of the channel state information, then it uses adaptive procedure to adjust the broadcast signal by adding the reverse of the channel such that when the channel effect takes place it can be highly reduced, and the signal arrives to the receiver with a very little noise which results in better performance. However, if the transmitter does not have perfect knowledge of the channel then the performance may get lower and in such a situation the receive diversity could result in better performance.

Spatial Multiplexing Vs Transmit and Receive Diversity:

Spatial multiplexing employs a minimum of two antennas at each side of the communication link and it does not employ any space time coding or precoding techniques, therefore its performance is unclear as it uses transmit and receive diversity implicitly with linear detection at the receiver. This work aims to address this problem, and for this purpose three linear detection algorithms; ZF, MMSE and ML have been implemented using different number of antennas. First, the performance of each algorithm (equations 1.27, 1.31, 1.34) for a 3*X*3 system is shown in Fig. 2.17:

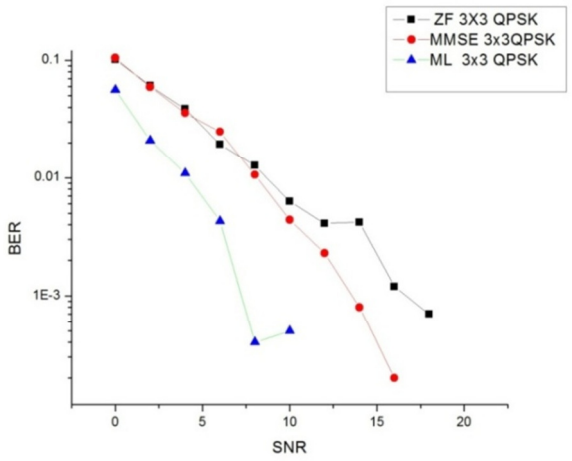

Figure 2.17 System performance of spatial multiplexing

The results of this work show that if the ZF and MMSE algorithms are applied to MIMO systems then at low SNR both algorithms show similar performance while at high SNR the MMSE shows better performance. This can be explained by looking back at the equations that express their noise powers which are listed here for convenience:

$$E\{||\tilde{\boldsymbol{Z}}_{\boldsymbol{ZF}}||^2\} = \sum_{i=1}^{N_T} \frac{\boldsymbol{\sigma_z}^2}{\boldsymbol{\sigma_i}^2}, \quad E\{||\tilde{\boldsymbol{Z}}_{\mathbf{MMSE}}||^2\} = \sum_{i=1}^{N_T} \frac{\boldsymbol{\sigma_z}^2\boldsymbol{\sigma_i}^2}{(\boldsymbol{\sigma_i}^2 + \boldsymbol{\sigma_z}^2)^2}$$

It is clear that at low SNR the variances of the noise ($\boldsymbol{\sigma_z}$) and signal ($\boldsymbol{\sigma_i}$) have close values which makes the noise powers in both algorithms close to each other and this manifests itself in a similar performance at low SNR, but as the SNR increases; the noise variance becomes lower and the noise powers of the former algorithms differ considerably which results in better performance in the MMSE approach. On the other hand, ML detection seems to have the highest performance because it does not work by minimizing the error presence in the received signal but rather by finding minimum distance between the received vector and a database of corresponding vectors, and in spite of the noise presence is still able to find the correct match because noise has a

limited effect in manipulating the distance between the original vector and the received vector. For this reason the ML approach appears to have an optimal performance. In order to find if the diversity order has an impact on the spatial multiplexing scheme, more number of antennas are added to both the transmitter and receiver sides (equations 1.27, 1.31, 1.34) and the results are shown in Fig. 2.18:

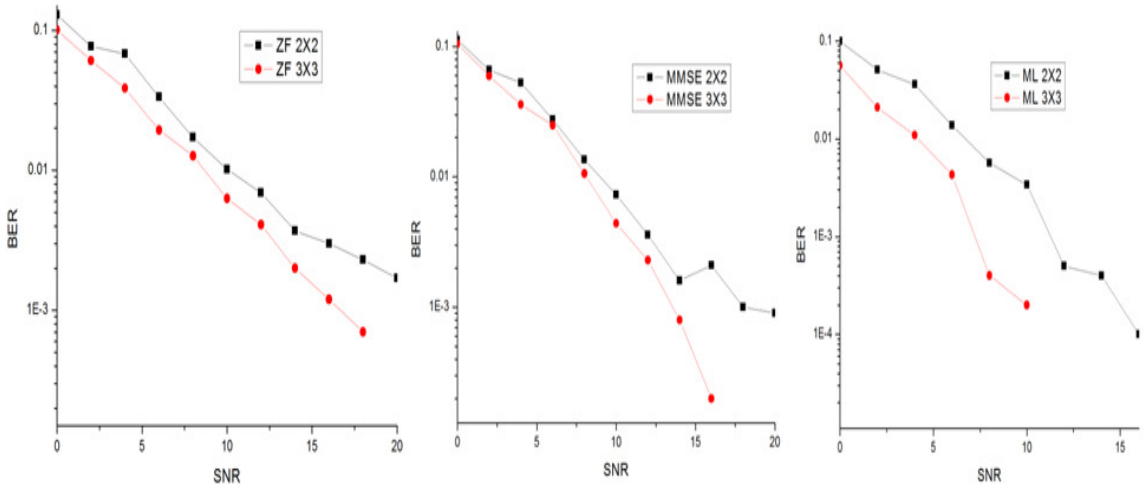

Figure 2.18 Spatial Multiplexing with increased diversity order

Increasing the diversity order corresponds to higher performance as can be seen from the above figure. However, this increase in performance seems to be moderate compared to the value of the diversity order which has been increased from 4 (in the 2*X*2 system) to 9 (in the 3*X*3 system) but yet the corresponding improvement seems to be lower than anticipated. To clarify the reason behind this behavior the receive diversity scheme has been shown in Fig. 2.19 with the rest of the former schemes:

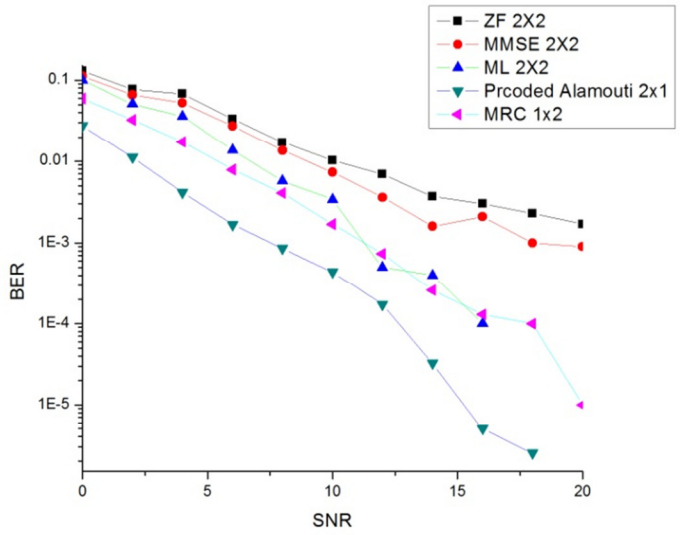

Figure 2.19 Receive diversity Vs Spatial Multiplexing

It is clear that receive diversity represented by MRC (equations 1.24, 1.25) falls in the same performance frame with the spatial multiplexing schemes (equations 1.27, 1.31, 1.34) particularly with ML detection. This can be understood by knowing that the receiver chains in the receive diversity and spatial multiplexing schemes are similar as both use similar combining and linear detection methods, consequently they appear to have close performance and it can be said that ML 2*X*2 and MRC 1*X*2 are almost the same except that there is one more antenna at the transmitter in the ML 2*X*2 scheme. As a result, increasing the number of antennas in the transmitter side does not have a tremendous impact overall on performance taking into account that space time coding is not used at the transmitter. This reveals an important fact about how transmit diversity actually works where increasing the number of antennas alone does not have a major effect if no space time coding is accompanied at each antenna. This is because the paths that each antenna provides to the signal will not be faded independently, but rather a correlation between them will take place and space time coding helps to break this

correlation. Therefore, increasing the number of antennas alone does not have a major contribution in mitigating the noise effect and providing better performance. On the other hand, the precoding method (equations 1.15-1.23) which depends on the knowledge of CSI is shown on the same figure and it proves to be the most powerful approach. This concludes the results of the key performance aspects of single user MIMO systems, and Fig. 2.20 shows additional comparisons where the SISO system shows the lowest performance among the rest of the schemes and adding more antennas to the receiver always results in a better noise mitigation.

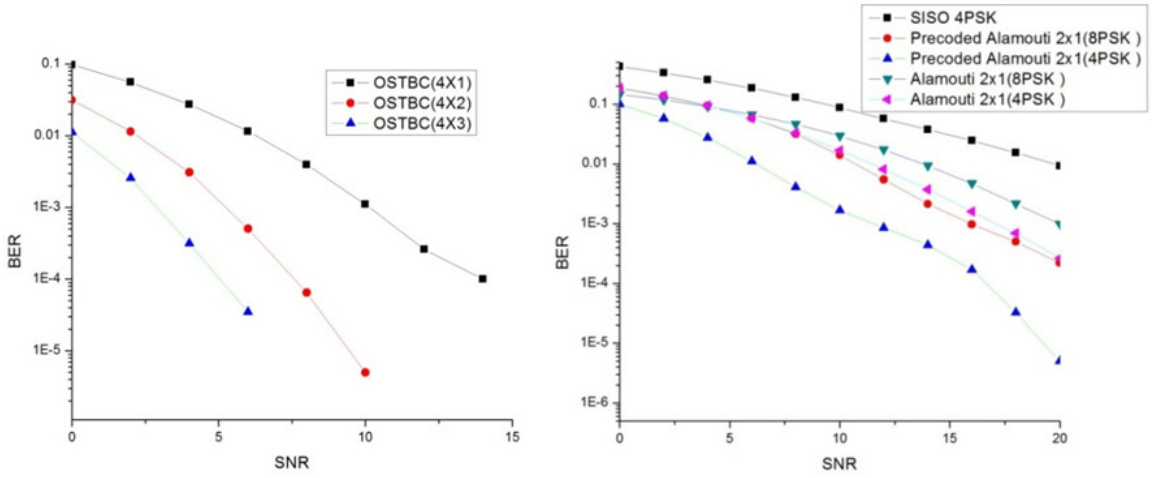

Figure 2.20 comparisons between different schemes

This work aims to find a mathematical formulation to describe the performance when the number of antenna elements is increased at the receiver side (equations 1.24-1.25). This helps predicting system performance when more antennas are employed at the receiver side for both the transmit and receive diversity schemes. In order to achieve this purpose, the SNR has been fixed at a constant value (2dB) while the number of antennas at the receiver has been increased, and the corresponding performance is recorded for both the transmit and receive diversity schemes. OriginPro mathematical modeling software has

been used to find the most accurate function that fits the obtained curve and the result of this modeling is shown in Fig. 2.21:

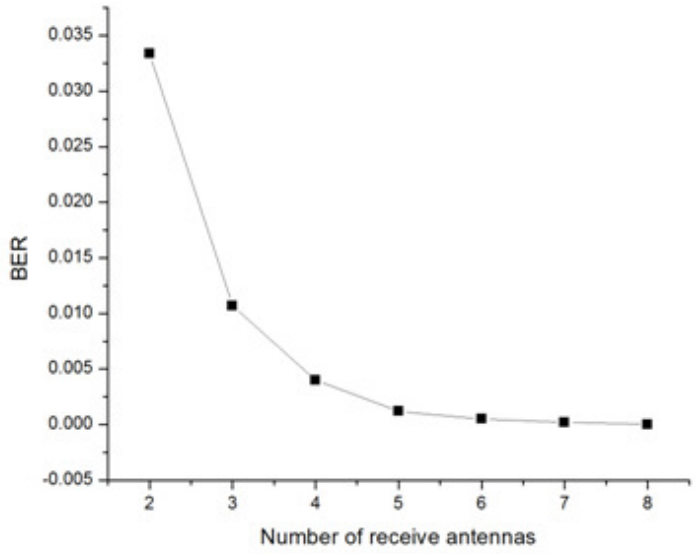

Figure 2.21. Performance using different number of antennas

According to the reported results, as the number of antenna elements increases at the receiver side the performance increases exponentially. In other words, the BER cure decreases with exponential behavior as shown in the above figure where the linear scale is considered instead of the logarithmic to visualize the effect. The reported exponential has the following form:

$$y = \exp(a + bx + cx^2)$$

Where y is the performance measure (BER in this case) x represents the number of antenna elements at the receiver and a, b, c are constants which depend on the channel conditions. Next, the same simulation has been run but with employing space time coding at the transmitter side (equations 1.15-1.23) to see the effect of the added transmit diversity gain and the result is shown in Fig. 2.22 below with logarithmic scaling:

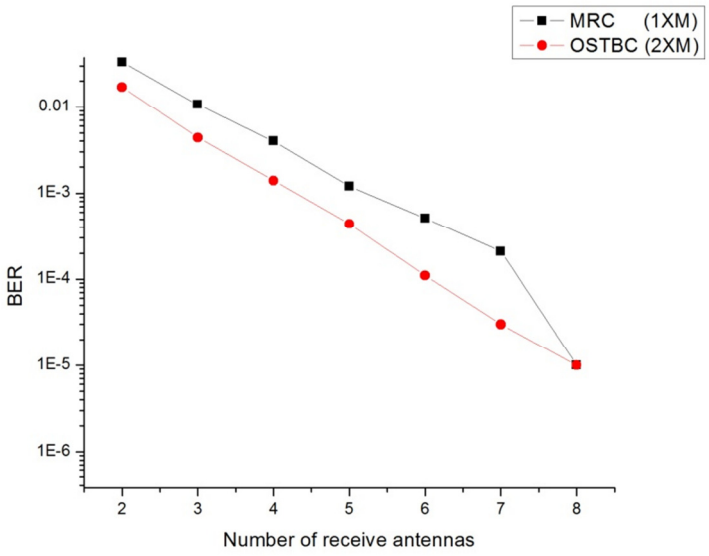

Figure 2.22 Effect of employing space time coding compared to MRC

As can be seen, the curve of MRC has been shifted downwards when space time coding is used indicating the importance of space time coding in transmit diversity.

Chapter 3: Multiuser MIMO Systems

Chapter Summary:

In the near future, leading carriers are moving to the Long Term Evolution (LTE) service that aims to provide more throughput and higher data rates by adopting MIMO systems as it is one of the key enablers of such improvements [25]. However, as more users need to be served by one Base Station; new problems emerge due to the need to detect multiple streams from different users at the same time. Therefore; different interference cancellation techniques needs to be adopted at the Mobile Station to overcome this problem because the single user techniques which were described in the last chapter lack interference suppression capabilities. In this chapter, five different algorithms are investigated and their performance is analyzed under similar conditions in order to find the optimum scheme which leads to the lowest interference possible. First, the basic theory of each technique is presented and then the results and findings of this work are listed.

3.1) Multiuser MIMO system model:

Figure 3.1 shows the system model for multiuser MIMO:

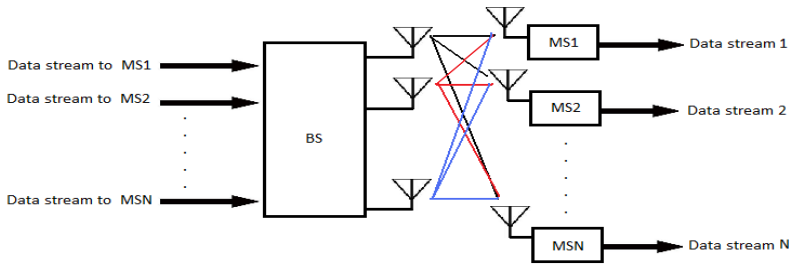

Figure 3.1 Multiuser MIMO system

3.1.1) Uplink Model (Multiple Access Channel):

The uplink model describes the data streams that are directed from MSs to a BS and it is called the Multiple Access Channel (MAC) [14]. Let $\boldsymbol{X}_u \in \mathbb{C}^{N_M X1}$be the transmitted signal from the u_{th}user where $u = 1,2, \dots, K$, and $\boldsymbol{Y}_{MAC} \in \mathbb{C}^{N_B X1}$be the received signal from all the K users assuming N_B is the number of antennas at the base station and N_M is the number of antennas at each mobile station, then the total received signal vector at the base station can be written as [14]:

$$\boldsymbol{Y}_{MAC} = \boldsymbol{H_u X_u} + \boldsymbol{Z} \Rightarrow \begin{bmatrix} \boldsymbol{Y_1} \\ \boldsymbol{Y_2} \\ \vdots \\ \boldsymbol{Y_K} \end{bmatrix} = [\boldsymbol{H_1} \quad \boldsymbol{H_2} \quad . \quad . \quad \boldsymbol{H_K}] \begin{bmatrix} \boldsymbol{X_1} \\ \boldsymbol{X_2} \\ \vdots \\ \boldsymbol{X_K} \end{bmatrix} + \boldsymbol{Z} \dots \dots \dots . (2.1)$$

Where: $\boldsymbol{H}_u \in \mathbb{C}^{N_B X N_M}$is the channel matrix between the u_{th} MS and the BS and $\boldsymbol{Z} \in \mathbb{C}^{N_B X1}$ is a noise matrix.

3.1.2) Downlink Model (Broadcast Channel):

The downlink model describes the data streams that are directed from a BS to MSs and it is called the Broadcast Channel (BC) [14]. Using the same assumptions for the MAC channel, the received signal vector can be expressed as [14]:

$$\boldsymbol{Y}_u = \boldsymbol{H_u X} + \boldsymbol{Z} \Rightarrow \begin{bmatrix} \boldsymbol{Y_1} \\ \boldsymbol{Y_2} \\ \vdots \\ \boldsymbol{Y_K} \end{bmatrix} = \begin{bmatrix} \boldsymbol{H_1} \\ \boldsymbol{H_2} \\ \vdots \\ \boldsymbol{H_K} \end{bmatrix} \boldsymbol{X} + \begin{bmatrix} \boldsymbol{Z_1} \\ \boldsymbol{Z_2} \\ \vdots \\ \boldsymbol{Z_K} \end{bmatrix} \dots \dots \dots . (2.2)$$

3.2) Transmission methods for the broadcast channel:

Here the methods for detecting data streams that are being broadcast to the MS which depend on the number of antennas at the receiving unit are investigated. The detection

methods used for the single antenna receivers are different from those for multiple antenna receivers and the reasons will be clarified next. In all coming treatments, the transmitter is always a BS and the receivers are MSs.

3.2.1) Single antenna receivers:

If the MS has only one receive antenna, then it will not be able to suppress any interference based on receive diversity principles. As a result, the transmitter needs to adopt precoding techniques to alleviate the interference effects [26] before transmission and this requires a perfect knowledge of the channel state information. There are four proposed methods to cancel the interference and noise effects for the single antenna receivers: dirty paper coding, Tomlinson and Harashima precoding, channel inversion and regularized channel inversion.

3.2.1.1) Dirty Paper Coding (DPC):

Caire and Shamai [7] proposed in 2001 an approach based on decomposing the channel matrix at the transmitter (assuming the channel is known to the transmitter) into an ordered set of interference channels such that the interference signal of the i_{th} user is generated as a linear combination of the signals transmitted in channels $j < i$ [7]. Assuming three users, let $\widetilde{\boldsymbol{X}} = [\tilde{X}_1\ \tilde{X}_2\ \tilde{X}_3]$ be the precoded vector of the data signal $\boldsymbol{X} = [X_1\ X_2\ X_3]$. Consequently, the received signal vector at the MS is given as [8]:

$$\boldsymbol{Y}_u = \boldsymbol{H_u}\widetilde{\boldsymbol{X}}_{\boldsymbol{u}} + \boldsymbol{Z} \Rightarrow \begin{bmatrix} Y_1 \\ Y_2 \\ Y_3 \end{bmatrix} = \begin{bmatrix} \boldsymbol{H_1} \\ \boldsymbol{H_2} \\ \boldsymbol{H_3} \end{bmatrix} \begin{bmatrix} \tilde{X}_1 \\ \tilde{X}_2 \\ \tilde{X}_3 \end{bmatrix} + \begin{bmatrix} Z_1 \\ Z_2 \\ Z_3 \end{bmatrix} \dots\dots\dots (2.3)$$

Where $\boldsymbol{H}_u \in \mathbb{C}^{1X3}$ is the channel matrix. Decomposing $\boldsymbol{H}_u$ to an upper triangular matrix **L** and orthonormal matrix **Q** using LU decomposition (Cholesky decomposition) gives [14]:

$$\boldsymbol{H_u = LQ} = \underbrace{\begin{bmatrix} l_{11} & 0 & 0 \\ l_{21} & l_{22} & 0 \\ l_{31} & l_{32} & l_{33} \end{bmatrix}}_{\boldsymbol{L}} \underbrace{\begin{bmatrix} q_1 \\ q_2 \\ q_3 \end{bmatrix}}_{\boldsymbol{Q}} \dots\dots\dots (2.4)$$

Transmitting $\boldsymbol{Q}^H\boldsymbol{X}$ through the channel eliminates $\boldsymbol{Q}$ due to the channel effect and we are left with $\boldsymbol{X}$. Therefore, the received signal vector can be rewritten as [14]:

$$\boldsymbol{Y}_u = \boldsymbol{LQQ}^H\boldsymbol{X} + \boldsymbol{Z} \Rightarrow \begin{bmatrix} Y_1 \\ Y_2 \\ Y_3 \end{bmatrix} = \begin{bmatrix} l_{11} & 0 & 0 \\ l_{21} & l_{22} & 0 \\ l_{31} & l_{32} & l_{33} \end{bmatrix} \begin{bmatrix} X_1 \\ X_2 \\ X_3 \end{bmatrix} + \begin{bmatrix} Z_1 \\ Z_2 \\ Z_3 \end{bmatrix} \dots\dots\dots (2.5)$$

- Signal received by user 1 is [14]:

$$Y_1 = l_{11}.X_1 + Z_1 \dots\dots\dots (2.6)$$

Where $l_{11}.X_1$is a scaled version of X_1. For interference free transmission we need [14]:

$$X_1 = \tilde{X}_1 \Rightarrow Y_1 = l_{11}.\tilde{X}_1 + Z_1 \dots\dots\dots (2.7)$$

- Signal received by user 2 [14]:

$$Y_2 = \underbrace{l_{21}.X_1}_{\textbf{Interference}} + \underbrace{l_{22}.X_2}_{\boldsymbol{Signal}} + \underbrace{Z_2}_{\boldsymbol{Noise}} = l_{21}.\tilde{X}_1 + l_{22}.X_2 + Z_2 \dots\dots\dots (2.8)$$

For interference free transmission we need [14]:

$$Y_2 = X_2 + Z_2 \dots\dots\dots (2.9)$$

This requires [14]:

$$X_2 = \tilde{X}_2 - \frac{l_{21}}{l_{22}} X_1 = \tilde{X}_2 - \frac{l_{21}}{l_{22}} \tilde{X}_1 \dots\dots\dots (2.10)$$

- Signal received by user 3 [14]:

$$Y_3 = \underbrace{l_{31}.X_1 + l_{32}.X_2}_{\textbf{Interference}} + \underbrace{l_{33}.X_3}_{\boldsymbol{Signal}} + \underbrace{Z_3}_{\boldsymbol{Noise}} \dots\dots\dots (2.11)$$

For interference free transmission we need [14]:

$$Y_3 = X_3 + Z_3 \dots\dots\dots (2.12)$$

This requires [14]:

$$X_3 = \tilde{X}_3 - \frac{l_{31}}{l_{33}} X_1 - \frac{l_{32}}{l_{33}} X_2 \dots\dots\dots (2.13)$$

From the above it can be seen that the precoding matrix for interference free transmission can be expressed as [14]:

$$\underbrace{\begin{bmatrix} X_1 \\ X_2 \\ X_3 \end{bmatrix}}_{\boldsymbol{Precoded}} = \begin{bmatrix} 1 & 0 & 0 \\ -\frac{l_{21}}{l_{22}} & 1 & 0 \\ -\frac{l_{31}}{l_{33}} + \frac{l_{32}}{l_{33}}\frac{l_{21}}{l_{22}} & -\frac{l_{32}}{l_{33}} & 1 \end{bmatrix} \underbrace{\begin{bmatrix} \tilde{X}_1 \\ \tilde{X}_2 \\ \tilde{X}_3 \end{bmatrix}}_{\boldsymbol{Signal}} \dots\dots\dots (2.14)$$

3.2.1.2) Tomlinson-Harashima Precoding (THP):

Fischer and others [8] proposed this technique in 2002 for MIMO systems where non-linear pre-equlization is performed at the transmitter to overcome the interference effect caused by the MIMO channel. Their approach is shown in Fig. 3.2:

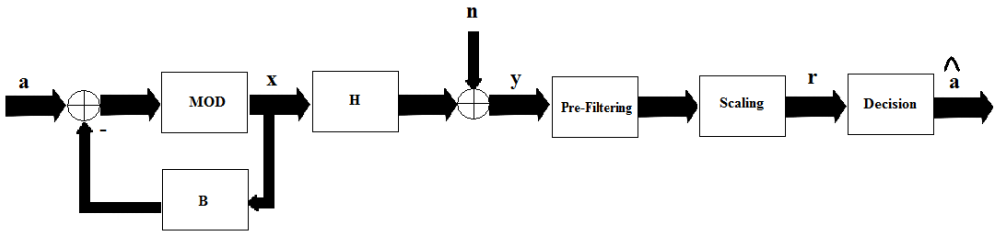

Figure 3.2 THP for MIMO channels

In this scheme the transmitted symbol $x_k$is expanded in order to achieve power saving because according to Shannon there is a tradeoff between power and bandwidth efficiency [27]. Therefore, expanding the constellation corresponds to the consumption of more bandwidth. Each symbol is expanded according to the following operation [14]:

$$c = MOD(x_k) = x_k + (m + jn) \dots\dots\dots (2.15)$$

Where m, n are chosen depending on the signal constellation. For M-ary PSK (where M is the number of points in the constellation) they are chosen as follows [8]:

$$m = 2\sqrt{M}d_I, \;\; n = 2\sqrt{M}d_Q \dots\dots\dots (2.16)$$

Where $d_I, d_Q$are the real and imaginary parts of the signal. The original symbol can be recovered by an opposite operation [14]:

$$x_k = MOD(c) = c - (m + jn) \dots\dots\dots (2.17)$$

Given the data symbols $\tilde{x}$, then the precoded symbols x^{TH} are found as [8]:

$$x_k^{TH} = MOD\left\{\tilde{x}_k - \sum_{l=1}^{k-1} b_{kl}.x_l^{TH}\right\} = \underbrace{\tilde{x}_k + m + jn}_{Expanded\ Symbol} - \sum_{l=1}^{k-1} b_{kl}.x_l^{TH} \dots\dots\dots (2.18)$$

$$k = 1,2,\dots.K.$$

Where b_{kl} is a feedback matrix that contains the CSI. Assuming three users and applying the LQ decomposition method on the channel response as in DPC [14]:

$$\boldsymbol{H_u = LQ} = \underbrace{\begin{bmatrix} l_{11} & 0 & 0 \\ l_{21} & l_{22} & 0 \\ l_{31} & l_{32} & l_{33} \end{bmatrix}}_{\boldsymbol{L}} \underbrace{\begin{bmatrix} q_1 \\ q_2 \\ q_3 \end{bmatrix}}_{\boldsymbol{Q}} \dots\dots\dots (2.19)$$

Then we find that the precoded data symbols can be expressed as [14]:

$$x_1{}^{TH} = mod(\tilde{x}_1) = \tilde{x}_1 \dots\dots\dots (2.20)$$

$$x_2{}^{TH} = mod\left(\tilde{x}_2 - \frac{l_{21}}{l_{22}} x_1{}^{TH}\right) = \tilde{x}_2 - \frac{l_{21}}{l_{22}}\tilde{x}_1 + 2A(m_2 + jn_2) \dots\dots\dots (2.21)$$

$$x_3{}^{TH} = mod\left(\tilde{x}_3 - \frac{l_{31}}{l_{33}} x_1{}^{TH} - \frac{l_{32}}{l_{33}} x_2{}^{TH}\right)$$

$$= \tilde{x}_3 - \frac{l_{31}}{l_{33}} x_1{}^{TH} - \frac{l_{32}}{l_{33}} x_2{}^{TH} + 2A(m_3 + jn_3) \dots\dots\dots (2.22)$$

Consequently, the received signal vector is [14]:

$$\begin{bmatrix} y_1 \\ y_2 \\ y_3 \end{bmatrix} = \begin{bmatrix} l_{11} & 0 & 0 \\ l_{21} & l_{22} & 0 \\ l_{31} & l_{32} & l_{33} \end{bmatrix} \begin{bmatrix} x_1{}^{TH} \\ x_2{}^{TH} \\ x_3{}^{TH} \end{bmatrix} + \begin{bmatrix} Z_1 \\ Z_2 \\ Z_3 \end{bmatrix} \dots\dots\dots (2.23)$$

- Signal received by user 1 [14]:

$$y_1 = x_1{}^{TH} l_{11} + Z_1 = \tilde{x}_1 l_{11} + Z_1 \dots\dots\dots (2.24)$$

- Signal received by user 2 [14]:

$$y_2 = l_{21}\tilde{x}_1 + l_{22} x_2{}^{TH} + Z_2 = l_{22}\tilde{x}_2 + l_{22} 2A(m_2 + jn_2) + Z_2 \dots\dots\dots (2.25)$$

By scaling and detection [14]:

$$\underbrace{\tilde{y}_2}_{Scaled} = \frac{y_2}{l_{22}} = \tilde{x}_2 + 2A(m_2 + jn_2) + \frac{Z_2}{l_{22}} \dots\dots\dots (2.26)$$

$$\underbrace{\hat{x}_2}_{Detected} = mod\left(\underbrace{\tilde{y}_2}_{Scaled}\right) = \tilde{x}_2 + \frac{Z_2}{l_{22}} \dots\dots\dots (2.27)$$

- Signal received by user 3 [14]:

$$y_3 = l_{31}{x_1}^{TH} + l_{32}{x_2}^{TH} + l_{33}{x_3}^{TH} + Z_3$$

$$y_3 = l_{33}\tilde{x}_3 + l_{33}.2A(m_3 + jn_3) + Z_3 \dots\dots\dots (2.28)$$

By scaling and detection [14]:

$$\underbrace{\tilde{y}_3}_{Scaled} = \frac{y_3}{l_{33}} = \tilde{x}_3 + 2A(m_3 + jn_3) + \frac{Z_3}{l_{33}} \dots\dots\dots (2.29)$$

$$\underbrace{\hat{x}_3}_{Detected} = mod\left(\underbrace{\tilde{y}_3}_{Scaled}\right) = \tilde{x}_3 + \frac{Z_3}{l_{33}} \dots\dots\dots (2.30)$$

3.2.2) Multiuser MIMO Channel Decomposition:

Another approach was proposed in 2004 by Choi and Murch [10] based on decomposing the multiuser channel into separate single user channels to cancel interference after that the channel inversion technique can be used to mitigate noise effects. This approach is shown in Fig. 3.3:

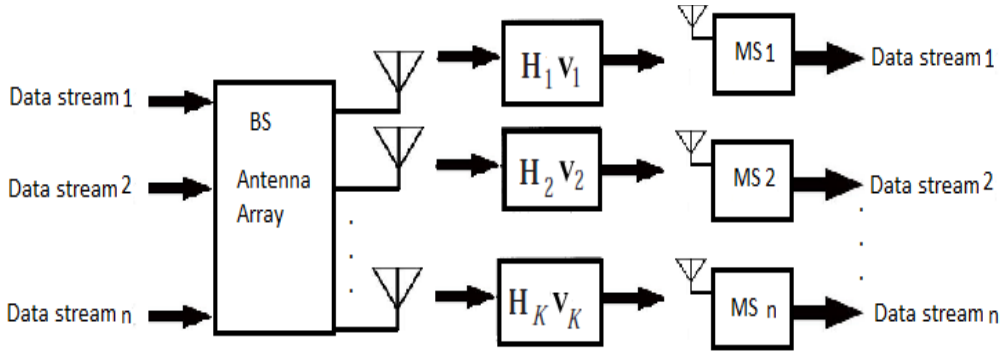

Figure 3.3 Multiuser MIMO decomposition

Let N_B be the number of transmit antennas at the BS, $N_{M,u}$is the number of receive antennas at each MS and K be the total number of users in the network. The data are pre-processed at the BS before transmission and the received signal vector in the u_{th} MS can be written as [14]:

$$\boldsymbol{y}_u = \boldsymbol{H}_u \sum_{k=1}^{K} \boldsymbol{w}_k \tilde{\boldsymbol{x}}_k + \boldsymbol{Z}_u = \underbrace{\boldsymbol{H}_u \boldsymbol{w}_u \tilde{\boldsymbol{x}}_u}_{Signal} + \underbrace{\sum_{k=1, k\neq u}^{K} \boldsymbol{H}_u \boldsymbol{w}_k \tilde{\boldsymbol{x}}_k}_{Interference} + \underbrace{\boldsymbol{Z}_u}_{Noise} \quad \ldots\ldots\ldots (2.31)$$

Where:

$\tilde{\boldsymbol{x}}_k$: The data symbol vector of user K

$\boldsymbol{w}_k$: The precoding matrix

$\boldsymbol{H}_u$: The channel matrix

$\boldsymbol{Z}_u$: The noise matrix

The aim is to make the interference term equals to zero by selecting none zero precoding matrices. This condition can be expressed as [14]:

$$\boldsymbol{H}_u \boldsymbol{w}_k = \mathbf{0}, \quad \forall u \neq k$$

For this purpose, a new channel matrix is constructed which contains the channel matrices of all users except the intended u_{th} user [14]:

$$\boldsymbol{H} = [\boldsymbol{H}_1{}^H \dots . \boldsymbol{H}^H{}_{u-1}\, \boldsymbol{H}^H{}_{u+1} \dots \dots . \boldsymbol{H}^H{}_k]^H \dots \dots \dots . (2.32)$$

Based on the proposed method in [10], by applying the singular value decomposition (SVD) on the matrix $\boldsymbol{H}$ we find [14]:

$$\boldsymbol{H} = \boldsymbol{U}[\boldsymbol{\Lambda}\ \mathbf{0}][\boldsymbol{V_1}\ \boldsymbol{V_2}]^H \dots \dots \dots . (2.33)$$

Using matrix operations, if both sides are multiplied by $\boldsymbol{V_2}$ we get [14]:

$$\boldsymbol{H V_2} = \boldsymbol{U}[\boldsymbol{\Lambda}\ \mathbf{0}] \begin{bmatrix} \boldsymbol{V_1} \\ \boldsymbol{V_2} \end{bmatrix}^H \boldsymbol{V_2} = \boldsymbol{U\Lambda}\, \underbrace{[\boldsymbol{V_1}]^H \boldsymbol{V_2}} = \boldsymbol{U\Lambda}\, \underbrace{\mathbf{0}} = \mathbf{0} \dots \dots \dots . (2.34)$$

Consequently, the best precoding matrix that cancels all the interference is $\boldsymbol{w}_u = \boldsymbol{V_2}$and this gives the following received signal vector assuming three users [14]:

$$\begin{bmatrix} \boldsymbol{y_1} \\ \boldsymbol{y_2} \\ \boldsymbol{y_3} \end{bmatrix} = \begin{bmatrix} \boldsymbol{H_1} & \boldsymbol{H_1} & \boldsymbol{H_1} \\ \boldsymbol{H_2} & \boldsymbol{H_2} & \boldsymbol{H_2} \\ \boldsymbol{H_3} & \boldsymbol{H_3} & \boldsymbol{H_3} \end{bmatrix} \begin{bmatrix} \boldsymbol{W_1}\widetilde{\boldsymbol{X}}_1 \\ \boldsymbol{W_2}\widetilde{\boldsymbol{X}}_2 \\ \boldsymbol{W_3}\widetilde{\boldsymbol{X}}_3 \end{bmatrix} + \begin{bmatrix} \boldsymbol{Z_1} \\ \boldsymbol{Z_2} \\ \boldsymbol{Z_3} \end{bmatrix} = \begin{bmatrix} \boldsymbol{H_1 W_1} & \boldsymbol{H_1 W_2} & \boldsymbol{H_1 W_3} \\ \boldsymbol{H_2 W_1} & \boldsymbol{H_2 W_2} & \boldsymbol{H_2 W_3} \\ \boldsymbol{H_3 W_1} & \boldsymbol{H_3 W_2} & \boldsymbol{H_3 W_3} \end{bmatrix} \begin{bmatrix} \widetilde{\boldsymbol{X}}_1 \\ \widetilde{\boldsymbol{X}}_2 \\ \widetilde{\boldsymbol{X}}_3 \end{bmatrix} + \begin{bmatrix} \boldsymbol{Z_1} \\ \boldsymbol{Z_2} \\ \boldsymbol{Z_3} \end{bmatrix}$$

$$\begin{bmatrix} \boldsymbol{y_1} \\ \boldsymbol{y_2} \\ \boldsymbol{y_3} \end{bmatrix} = \begin{bmatrix} \boldsymbol{H_1 W_1} & \mathbf{0} & \mathbf{0} \\ \mathbf{0} & \boldsymbol{H_2 W_2} & \mathbf{0} \\ \mathbf{0} & \mathbf{0} & \boldsymbol{H_3 W_3} \end{bmatrix} \begin{bmatrix} \widetilde{\boldsymbol{X}}_1 \\ \widetilde{\boldsymbol{X}}_2 \\ \widetilde{\boldsymbol{X}}_3 \end{bmatrix} + \begin{bmatrix} \boldsymbol{Z_1} \\ \boldsymbol{Z_2} \\ \boldsymbol{Z_3} \end{bmatrix} \dots \dots \dots . (2.35)$$

This way the multiuser MIMO channel has been decomposed to single user MIMO channels [10].

3.3) Channel Inversion:

This method cancels the channel effect by multiplying the data stream with the opposite channel response at the transmitter such that the channel effect is cancelled when the signal arrives to the receiver [26]. For this reason, the CSI must be perfectly known to the receiver which feeds this information back to the transmitter. Figure 3.4 shows this technique:

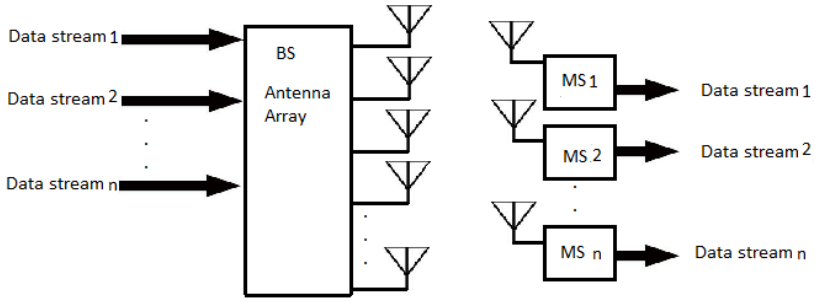

Figure 3.4 Channel Inversion

Based on the above figure the transmitted signal can be written as [26]:

$$\boldsymbol{S} = \frac{1}{\sqrt{\gamma}} \boldsymbol{H}^H (\boldsymbol{H}\boldsymbol{H}^H)^{-1} \boldsymbol{d} \ldots\ldots\ldots (2.36)$$

Where $\boldsymbol{d}$ is the data signal vector**,** **H** is the channel matrix**,** and γ is a scaling factor to limit the total transmitted power. The symbol$(.)^H$ denotes the Hermitian transpose. At the receiver, only the desired signal is seen with additive Gaussian noise and this can be expressed as [26]:

$$x_j = \frac{1}{\sqrt{\gamma}} \underbrace{d_j}_{Data} + \underbrace{e_j}_{Noise} \ldots\ldots\ldots (2.37)$$

3.4) Regularized Channel Inversion:

Peel and others [9] proposed in 2005 a technique that regularizes the inverse of the channel response through the addition of identity matrix before inverting as follows [9]:

$$\boldsymbol{S} = \boldsymbol{H}^H(\boldsymbol{H}\boldsymbol{H}^H + \alpha \boldsymbol{I}_K)^{-1}\boldsymbol{u} \dots\dots\dots (2.38)$$

Where: $\boldsymbol{u}$ is the transmitted signal vector. After going through the channel, the (un-normalized) signal at the receiver can be expressed as [9]:

$$\boldsymbol{H}\boldsymbol{S} = \boldsymbol{H}\boldsymbol{H}^H(\boldsymbol{H}\boldsymbol{H}^H + \alpha \boldsymbol{I}_K)^{-1}\boldsymbol{u} \dots\dots\dots (2.39)$$

By using the singular value decomposition (SVD) $\boldsymbol{H}\boldsymbol{H}^H = \boldsymbol{Q}\boldsymbol{\Lambda}\boldsymbol{Q}^H$, the former equation can be rewritten as [9]:

$$\boldsymbol{H}\boldsymbol{S} = \boldsymbol{Q}\frac{\boldsymbol{\Lambda}}{\boldsymbol{\Lambda} + \alpha \boldsymbol{I}}\boldsymbol{Q}^H\boldsymbol{u}$$

$$= \left[q_{k,1}\frac{\lambda_1}{\lambda_1 + \alpha} \dots . q_{k,K}\frac{\lambda_k}{\lambda_k + \alpha}\right]\begin{bmatrix} {q_{1,1}}^H & \cdots & {q_{k,1}}^H \\ \vdots & \ddots & \vdots \\ {q_{1,k}}^H & \cdots & {q_{k,k}}^H \end{bmatrix}\begin{bmatrix} u_1 \\ . \\ . \\ u_k \end{bmatrix} \dots\dots\dots (2.40)$$

Where $q_{k,l}$is the $(q_{k,l})_{th}$entry of the matrix $\boldsymbol{Q}$. The un-normalized desired signal term is [9]:

$$\left(\sum_{l=1}^{k}\frac{\lambda_l}{\lambda_l + \alpha}\left|q_{k,l}\right|^2\right)u_k$$

Where λ is the eigenvalue of $\boldsymbol{H}\boldsymbol{H}^H$. All the remaining terms $u_l(l \neq k)$ represent interference terms and they must be cancelled in order to get an interference free signal for the K_{th} user which can be expressed as [9]:

$$y_k = \frac{1}{\sqrt{\gamma}}\left(\sum_{l=1}^{k}\frac{\lambda_l}{\lambda_l+\alpha}\left|q_{k,l}\right|^2\right)u_k + w_k' \ldots\ldots\ldots (2.41)$$

Where: w_k'combines noise and interference effects. In order to achieve this, the optimum value of α needs to be found such that the signal to noise plus interference ratio is maximized [9]:

$$SINR \approx \frac{\left(\sum_{l=1}^{K}\frac{\lambda_l}{\lambda_l+\alpha}\right)^2}{\sigma^2K^2\sum_{l=1}^{K}\frac{\lambda_l}{(\lambda_l+\alpha)^2} + K\sum_{l=1}^{K}\left(\frac{\lambda_l}{\lambda_l+\alpha}\right)^2 - \left(\sum_{l=1}^{K}\frac{\lambda_l}{\lambda_l+\alpha}\right)^2} \ldots\ldots\ldots (2.42)$$

After some mathematics it can be shown that the optimum value of α which maximizes the above SINR is [9]:

$$\alpha = K\sigma^2 = \frac{K}{\rho} \ldots\ldots\ldots (2.43)$$

Where K is the number of users and $\sigma^2$is the noise power.

3.5) Multiple antenna receivers:

If the receiver has more than one antenna, then the multiuser MIMO channel is decomposed to independent single user MIMO channels and afterwards any of the space diversity techniques can be used to mitigate noise and multipath fading.

3.6) Results and Findings:

In this work it is assumed that there is a maximum of 11 users in the network, all of them are stationary not moving. The base station is broadcasting different data streams for each user in a multipath fading environment and the channel state information is known to the

transmitter. First, the channel and regularized channel inversion algorithms (equations 2.36-2.37, 2.38-2.43) are simulated and their performance is shown in Fig. 3.5 below for different number of users in the network:

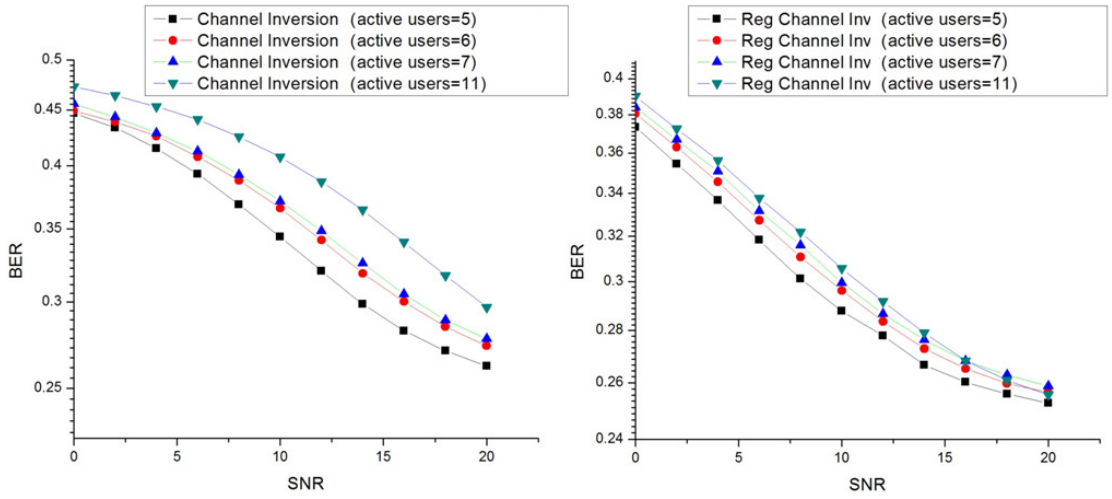

Figure 3.5 Multiuser MIMO system performance using channel inv and reg channel inv

It is obvious that in both cases the performance degrades as the number of users increases in the network because the level of interference becomes higher. In Fig. 3.6 the performance of both algorithms is shown for 11 users for the sake of comparison:

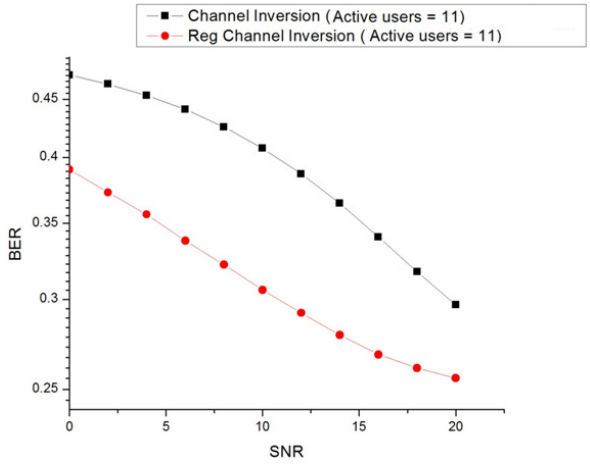

Figure 3.6 Comparison between channel inversion and regularized channel inversion

It is clear from the former figures that the regularized channel inversion offers higher performance compared to the channel inversion and this improvement is due to the added factor α that maximizes the signal to noise ratio. Second, the DPC (equations 2.3-2.14) and THP (equations 2.15-2.30) algorithms are implemented under the same conditions for different number of users and the results are shown in Fig. 3.7:

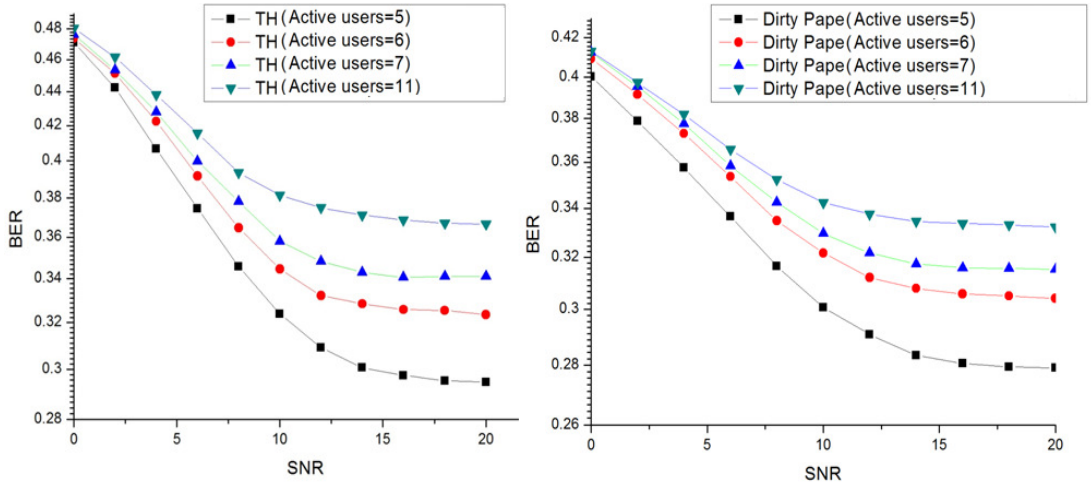

Figure 3.7 Multiuser MIMO system performance using DPC and THP

In Fig. 3.8 a comparison between the former two schemes is shown for 5 users:

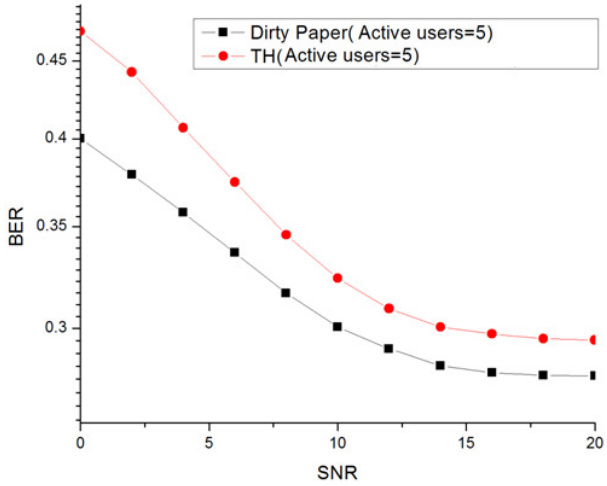

Figure 3.8 Comparison between DPC and THP

The reported result is interesting, although the THP consumes more bandwidth it shows lower performance compared to DPC which conserves the bandwidth of the system. The difference in their performance seems to be higher at low SNR but as the SNR increases their performance becomes closer. It is expected that as long as both algorithms use the same precoding method which is based on the channel decomposition approach and THP consumes more spectral bandwidth, then THP shall have better performance but the results show the opposite. This can be explained by the way THP manipulates the constellation of the signal in order to achieve power conservation. In THP the constellation is expanded at the transmitter side before the signal is sent to the receiver. This expansion changes the original locations of the I and Q components of the signal which increases the probability of erroneous recovery especially after the noise is added to the signal which results in more deviation from the original locations of the constellation points. In order to make a fair judgment concerning the optimal scheme of the single antenna receivers, the algorithms are implemented where the same number of users is considered under the same noise and fading conditions and the results are shown in Fig. 3.9:

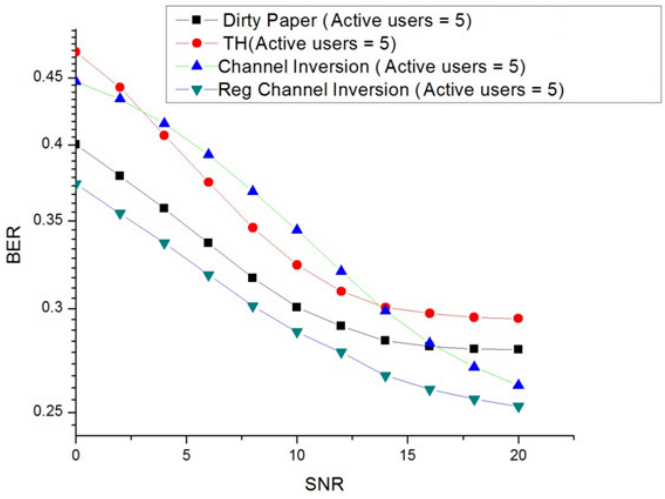

Figure 3.9. Comparison between the single antenna detection algorithms

The findings of the work show that the regularized channel inversion (equations 2.38-2.43) approach has superior performance among the rest of the proposed algorithms. The reason behind this performance can be understood by fact that although regularized channel inversion requires perfect knowledge of the channel state information like the rest of the schemes, it does not aim to decompose the channel using Cholesky decomposition as in DPC and THP which has high approximation errors, but rather it uses the SVD decomposition method which gives better approximation to the channel matrix which has a strong impact on the system performance. This has been reported for a different application by [28]; where it has been shown that Cholesky decomposition has more roundoff errors in comparison with SVD. Moving to the multiple antenna receivers, this work investigated the multiple antenna receivers approach for two users and each user has a MS with two antennas and spatial multiplexing is employed at the receiver chain with ML detection (equation 1.34) after the channel is decomposed (equations 2.31-2.35). The results are compared with the regularized channel inversion and shown in Fig. 3.10 below:

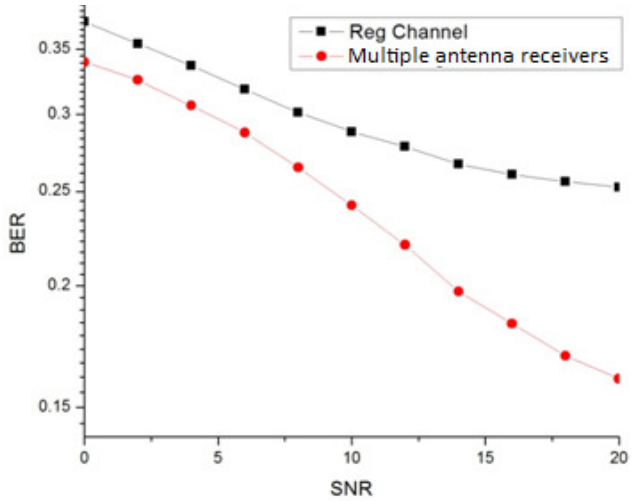

Figure 3.10. Multiple antenna receivers and Reg channel inversion

Using two antennas at the receiver with ML detection gives better performance compared to the proposed single antenna algorithms. This shows that in general multiple antenna receivers shall result in higher performance compared to single antenna receivers because space diversity gain becomes available.

Chapter 4: MIMO Systems using Beamforming

Chapter Summary:

In the previous chapters the single user and multiuser MIMO schemes were investigated. All of those schemes use omnidirectional antennas where the antenna elements radiate in all directions with no beam directivity. In this chapter the performance of MIMO systems is evaluated using antenna arrays where directional beams are formed to the intended users and nulls are formed in the direction of interference. The major contribution of this work is presented in this chapter where four different techniques widely used in different signal processing applications: phased arrays, LCMV, MVDR and Frost algorithms are applied to MIMO systems for the sake of investigating the wireless system performance using beamforming. First, the basic theory of each algorithm is presented then a communication system is implemented for each one and different performance aspects are evaluated.

4.1) Phased Arrays:

Phased arrays have the ability to provide high beam gains which has a lot of advantages in applications like radar, sonar and imaging [13]. Incorporating phased arrays in MIMO systems shall bring a major advantage to the wireless communication systems represented by the capability of spatial filtering which gives phased arrays high potential to suppress all signals coming from undesired directions [29]. On the other hand, spatial filtering can be used to alleviate the problem of fading and multichannel interference as well [30].

- Phased array transmitter:

Phased arrays form a phase shift beamformer and it is mainly used for narrow band applications [31]. It can be employed at both the transmitter and receiver for the sake of boosting system performance. Omnidirectional transmitters radiate power in all directions and only a small portion of the emitted power gets to the receiver while the rest form an interference source for other receivers in the network [29]. On the other hand, phased arrays allow most of the radiated power to be steered in the desired direction which boosts the maximum range of communication without increasing the power level as shown in Fig. 4.1:

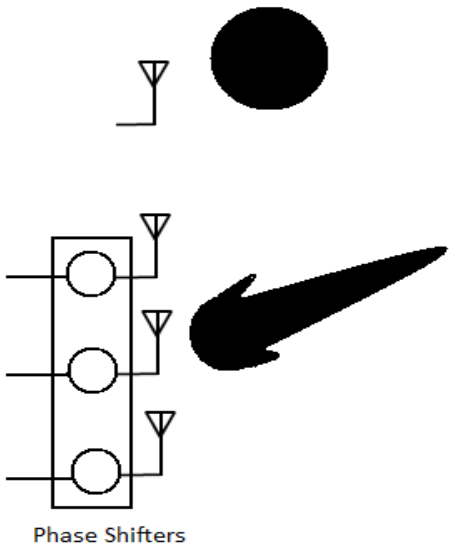

Figure 4.1 Phased array transmitter

The radiation pattern of the array is found by multiplying the radiated pattern of a single antenna element by the array factor [29]. To clarify this point; consider a one directional array of M elements as shown in Fig. 4.2:

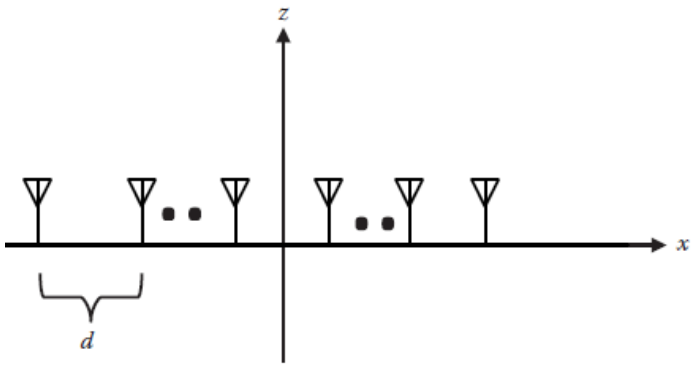

Figure 4.2 Linear array of N elements

The elements are uniformly spaced with a spacing of *d* and centered around $x = 0$, their position can be written as [13]:

$$x_m = [m - 0.5(1 + M)]d, \quad m = 1,2, \ldots, M. \quad \ldots\ldots\ldots (3.1)$$

The array factor represents the spatial response and is given as the coherent sum of the element voltages and can be expressed as follows (assuming no phase steering) [13]:

$$AF = \sum_{m=1}^{M} A_m e^{j\frac{2\pi}{\lambda}x_m \sin\theta} \ldots\ldots\ldots (3.2)$$

Where: θ is the angle of incidence and λ is the wavelength. The radiation pattern is given as [13]:

$$F(\theta) = EPxAF = EP \sum_{m=1}^{M} A_m e^{j\frac{2\pi}{\lambda}x_m \sin\theta} = \cos^{\frac{EF}{2}} \sum_{m=1}^{M} A_m e^{j\frac{2\pi}{\lambda}x_m \sin\theta} \ldots\ldots\ldots (3.3)$$

Where EP is the element pattern and it is represented as a cosine function raised to a power that is called the element factor EF. The former pattern has a maximum value at $\theta = 0$. In order to steer the array to have a maximum in a different direction, the phase of

each element needs to be adjusted by a weight that modifies both the voltage and phase as follows [13]:

$$W = A_m = a_m e^{j\theta_m} \dots\dots\dots (3.4)$$

Then the steered radiation pattern can be written as [13]:

$$F(\theta) = \cos^{\frac{EF}{2}} \sum_{m=1}^{M} \underbrace{a_m e^{j\theta_m}}_{Weight} e^{j\frac{2\pi}{\lambda} x_m \sin\theta} \dots\dots\dots (3.5)$$

Where $\theta_m$is [13]:

$$\theta_m = -\frac{2\pi}{\lambda} x_m \sin\theta_o \Rightarrow F(\theta) = \cos^{\frac{EF}{2}} \sum_{m=1}^{M} a_m e^{j(\frac{2\pi}{\lambda} x_m \sin\theta - \frac{2\pi}{\lambda} x_m \sin\theta_o)} \dots\dots\dots (3.6)$$

Each element has a phase shifter to apply the appropriate weights in order to steer the main beam in the desired directions [13].

- Phased array receiver:

Phased arrays can be incorporated at the receiver side as shown in Fig. 4.3:

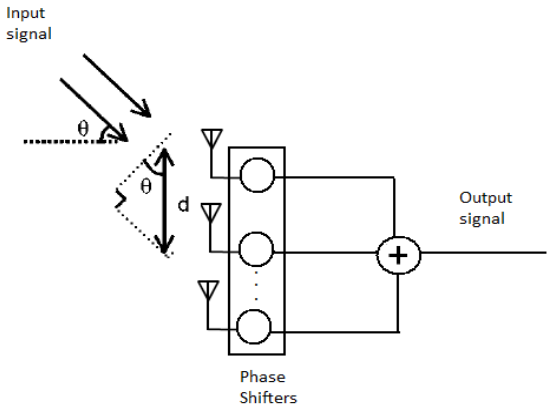

Figure 4.3 Phased array receiver

To find the improved signal, we start by finding the time delay between two adjacent antenna elements as follows [32]:

$$\tau = \frac{d\sin(\theta)}{c} \ldots\ldots\ldots (3.7)$$

Where d and c are the element spacing and the speed of light respectively. The received signal by the first antenna element is [32]:

$$s_o(t) = A(t)Cos(2\pi ft + \varphi(t)) \ldots\ldots\ldots (3.8)$$

The received signal by the n_{th}antenna element is [32]:

$$s_i(t) = s_o(t - n\tau) = A(t - n\tau)Cos(2\pi f(t - n\tau) + \varphi(t - n\tau)) \ldots\ldots\ldots (3.9)$$

Where $A(t)$ and $\varphi(t)$ are the gain and phase of the signal respectively and f is the carrier frequency. After appropriate weighting we get [32]:

$$A(t) = A(t - n\tau), \quad \varphi(t) = \varphi(t - n\tau), \quad \emptyset_n = n\emptyset = 2\pi f\tau n \ldots\ldots\ldots (3.10)$$

The combined signal is given as [32]:

$$s_{out} = \sum_{n=0}^{N-1} A(t - n\tau)\, Cos(2\pi ft + \varphi(t - n\tau) - 2\pi nf\tau + \emptyset_n) \ldots\ldots\ldots (3.11)$$

$$s_{out} = \sum_{n=0}^{N-1} A(t)\, Cos(2\pi ft + \varphi(t) - 2\pi nf\tau + \emptyset_n) = N.s_o(t) \ldots\ldots\ldots (3.12)$$

This shows that signals which arrive at each antenna element can be added coherently to give an improved signal gain at the output of the receiver [32].

4.2) MVDR Beamformer:

The minimum variance distortionless response (MVDR) beamformer is one of the adaptive optimum statistical beamformers which assurers a distortionless response for a predefined steering direction [33]. In this section the principles of the MVDR beamformer are presented and analyzed in order to find the optimal weights that give improved performance. Let's consider a received plane wave signal which can be written in the frequency domain representation using vector notation as [12]:

$$\boldsymbol{X}(w) = \boldsymbol{X_s}(w) + \boldsymbol{N}(w) \dots \dots \dots . (3.13)$$

Where $\boldsymbol{X_s}(w)$ is the received signal array and $\boldsymbol{N}(w)$ is a zero mean random noise vector. The transmitted signal vector $\boldsymbol{X_s}(w)$ can be decomposed into a transmitted signal vector $\boldsymbol{F}(w)$ and array manifold vector called the steering vector $\boldsymbol{V}(w: K_s)$ as follows [12]:

Transmitted Signal Vector = Information Signal Vector X Steering Vector

$$\Rightarrow \boldsymbol{X_s}(w) = \boldsymbol{F}(w).\boldsymbol{V}(w: \boldsymbol{K_s}) \Rightarrow \boldsymbol{X}(w) = \boldsymbol{F}(w).\boldsymbol{V}(w: \boldsymbol{K_s}) + \boldsymbol{N}(w) \dots \dots \dots . (3.14)$$

Where: w and K_s are the frequency and the wave number respectively. On the other hand, the noise has the following spectral matrix [12]:

$$\boldsymbol{S}_n(w) = \boldsymbol{S}_c(w) + {\sigma_w}^2 \boldsymbol{I} \dots \dots \dots . (3.15)$$

Where $\boldsymbol{S}_n$ is the noise covariance matrix. The output of the weight processor is shown in Fig. 4.4 and is given as [12]:

$$\boldsymbol{Y}(w) = \boldsymbol{W^H}(w).\boldsymbol{X}(w) = \boldsymbol{F}(w) + \boldsymbol{Y_n}(w), \text{ For distortion free response}$$

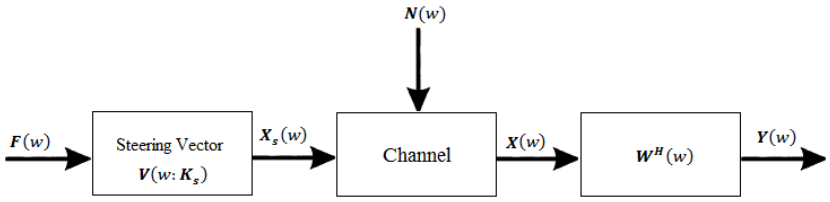

Figure 4.4 Block diagram of the MVDR beamforming

Where: $\boldsymbol{F}(w)$and $\boldsymbol{Y_n}(w)$ are the original signal vector and a white Gaussian noise respectively and $\boldsymbol{W^H}$is 1XN weight vector. For clarification, the former equations can be rewritten as follows [12]:

$$\boldsymbol{Y}(w) = \boldsymbol{W^H}(w).\boldsymbol{X}(w) = \boldsymbol{W^H}(w)[\boldsymbol{X_s}(w) + \boldsymbol{N}(w)] = \boldsymbol{W^H}(w)[\boldsymbol{F}(w).\boldsymbol{V}(w{:}\,\boldsymbol{K_s}) + \boldsymbol{N}(w)]$$

$$\boldsymbol{Y}(w) = \boldsymbol{W^H}(w)[\boldsymbol{F}(w)\boldsymbol{V}(w{:}\,\boldsymbol{K_s}) + \boldsymbol{S}_n(w)] = \boldsymbol{F}(w)\boldsymbol{W^H}(w).\boldsymbol{V}(w{:}\,\boldsymbol{K_s}) + \boldsymbol{W^H}(w).\boldsymbol{S}_n(w)$$

$$\Rightarrow \boldsymbol{Y}(w) = \boldsymbol{F}(w).\boldsymbol{W^H}(w).\boldsymbol{V}(w{:}\,\boldsymbol{K_s}) + \boldsymbol{Y_n}(w) \dots\dots\dots (3.16)$$

Where: $\boldsymbol{Y_n}(w) = \boldsymbol{W^H}(w).\boldsymbol{S}_n(w)$

- **Distortionless Criterion:**

For distortion free response this requires [12]:

$$\boldsymbol{Y}(w) = \boldsymbol{F}(w) \dots\dots\dots (3.17)$$

Consequently this needs [12]:

$$\boldsymbol{W^H}(w).\boldsymbol{V}(w{:}\,\boldsymbol{K_s}) = 1 \dots\dots\dots (3.18)$$

Because [12]:

$$\boldsymbol{Y}(w) = \boldsymbol{F}(w).\underbrace{\boldsymbol{W^H}(w).\boldsymbol{V}(w{:}\,\boldsymbol{K_s})} + \boldsymbol{Y_n}(w) = \boldsymbol{F}(w).\underbrace{1} + \boldsymbol{Y_n}(w) \dots\dots\dots (3.19)$$

It also requires minimizing the noise power which is given as [12]:

$$E[|\boldsymbol{Y_n}(w)|^2] = \boldsymbol{W^H}(w).\boldsymbol{S}_n(w).\boldsymbol{W}(w) \dots \dots \dots (3.20)$$

Therefore, two conditions must be met which are called criterion and constraint such that [12]:

Criterion: minimize $E[|\boldsymbol{Y_n}(w)|^2]$; subject to the Constraint: $\boldsymbol{W^H}(w).\boldsymbol{V}(w{:}\,\boldsymbol{K_s}) = 1$

One useful method to solve this problem is Lagrange multipliers which is a method for finding the local maxima and minima of a function subject to equality constraints [34]. A new variable λ called Lagrange multiplier is introduced to form the Lagrangian which is given as [34]:

$$F(x, y, \lambda) = f(x, y) + \lambda[g(x, y) - c] \dots \dots \dots (3.21)$$

Where in this case:

$$\text{Minimize: } f(x, y) \Leftrightarrow E[|\boldsymbol{Y_n}(w)|^2] = \boldsymbol{W^H}(w).\boldsymbol{S}_n(w).\boldsymbol{W}(w) \dots \dots \dots (3.22)$$

$$\text{Subject to: } g(x, y) = c \Leftrightarrow \boldsymbol{W^H}(w).\boldsymbol{V}(w{:}\,\boldsymbol{K_s}) = 1 \dots \dots \dots (3.23)$$

$$\text{Where: } g(x, y) \Leftrightarrow \boldsymbol{W^H}(w).\boldsymbol{V}(w{:}\,\boldsymbol{K_s}), \qquad c = 1 \dots \dots \dots (3.24)$$

The aim is to find the weights $\boldsymbol{W^H}(w)$ that minimize F. After some mathematics those weights can be found as [12]:

$$\boldsymbol{W^H}(w) = \boldsymbol{\Lambda}(w{:}\,\boldsymbol{K_s}).\boldsymbol{V^H}(w{:}\,\boldsymbol{K_s}).\boldsymbol{S}_n(w)^{-1} \dots \dots \dots (3.25)$$

$$\text{Where: } \boldsymbol{\Lambda}(w{:}\,\boldsymbol{K_s}) = [\boldsymbol{V^H}(w{:}\,\boldsymbol{K_s}).\boldsymbol{S}_n(w)^{-1}.\boldsymbol{V}(w{:}\,\boldsymbol{K_s})]^{-\boldsymbol{1}} \dots \dots \dots (3.26)$$

4.3) LCMV Beamformer:

This type of beamformer imposes more constraints on the beamformer characteristics in cases where unexpected change of the working conditions takes place such as changing the supposed angle of arrival where the desired signal arrives from a different angle. For this purpose some linear constrains can be imposed to control the behavior of the beamformer. The general form for a constraint condition can be expressed as:

Weight Vector X Constraints = Intended Result Response

This can be formulated as follows [12]:

$$\boldsymbol{W^H}.\boldsymbol{C} = \boldsymbol{g^H} \text{ or } \boldsymbol{C^H}.\boldsymbol{W} = \boldsymbol{g} \dots\dots\dots (3.27)$$

The aim is to find the weights matrix $\boldsymbol{W^H}$ that makes $\boldsymbol{C}$ and $\boldsymbol{g}$ equal to each other. The linear constraint minimum variance (LCMV) beamformer minimizes the noise power as in the MVDR case but subject to a set of more constraints $\boldsymbol{W^H}.\boldsymbol{C} = \boldsymbol{g^H}$ [12]. Here two types of constraints are imposed; the same distortionless constraint of the MVDR beamformer in addition to a directional constraint to overcome the DoA mismatch, and the aim is to find a set of weights $\boldsymbol{W^H}$ that satisfies those constraints. Starting from the input signal to the beamformer which can be written as [12]:

$$\boldsymbol{X}(w) = \boldsymbol{V}.\boldsymbol{F}(w) + \boldsymbol{N}(w) \dots\dots\dots (3.28)$$

Where: $\boldsymbol{F}$ and $\boldsymbol{V}$are the information signal and the steering vectors respectively and $\boldsymbol{N}$ is a white Gaussian noise vector. The output signal is given as [12]:

$$\boldsymbol{Y}(w) = \boldsymbol{W^H}(w).\boldsymbol{X}(w) \dots\dots\dots (3.29)$$

Next the following constraints are imposed:

- Distortionless constraint:

This is the same constraint of the MVDR beamformer which can be written as [12]:

$$\boldsymbol{W^H}(w).\boldsymbol{V}_{\text{Mismatch}} = 1 \dots \dots \dots . (3.30)$$

Where $\boldsymbol{V}_{\text{Mismatch}}$ is a steering vector with a DoA mismatch from the desired direction.

- Directional constraint:

To rectify the DOA mismatch problem a constraint on the steering vector is imposed [12]:

$$\boldsymbol{W^H}(w).\boldsymbol{V}(K_i) = \boldsymbol{g}_i \dots \dots \dots . (3.31)$$

Where $\boldsymbol{g}_i$is the value of the constraint and K_i denotes the wavenumber along the desired $\boldsymbol{g}_i$. To avoid the DoA mismatch problem, beam directivity is required in the desired direction $\psi_m$with $\pm\Delta\psi_m$mismatch tolerance and this can be expressed as [12]:

$$\boldsymbol{W^H V}(\psi_m) = 1, \qquad \boldsymbol{W^H V}(\psi_m + \Delta\psi_m) = 1, \qquad \boldsymbol{W^H V}(\psi_m - \Delta\psi_m) = 1 \dots \dots . (3.32)$$

This can be written in a matrix notation as follows [12]:

$$\boldsymbol{W^H}.\boldsymbol{C} = \boldsymbol{g^H} \quad \text{Where: } \boldsymbol{C} = [\boldsymbol{V}(\psi_m)\ \boldsymbol{V}(\psi_m + \Delta\psi_m)\ \boldsymbol{V}(\psi_m - \Delta\psi_m)],\ \boldsymbol{g} = \begin{bmatrix}1\\1\\1\end{bmatrix} \dots . (3.33)$$

- Null constraints:

Assuming there is a jamming signal coming from a known direction, a constraint condition needs to be imposed on the steering vector that put nulls in the direction of interferers. This can be expressed as [12]:

$$\boldsymbol{W^H}(w).\boldsymbol{V}(K_1) = 1 \dots \dots \dots . (3.34) \text{ (Desired direction)}$$

$$\boldsymbol{W^H}(w).\boldsymbol{V}(K_i) = 0, \;\; i = 2,3, \dots , M_0 \dots \dots \dots . (3.35) \text{ (Interferers)}$$

Thus [12]:

$$\boldsymbol{C} = [\boldsymbol{V_1}_{\text{desired}} \;\; \boldsymbol{V_2}_{\text{Intf}} \;\; \boldsymbol{V_3}_{\text{Intf}} \;\; \boldsymbol{V_4}_{\text{Intf}} \dots \dots \dots \dots \;\; \boldsymbol{V_{M_0}}_{\text{Intf}}] \;\; ,$$

$$\boldsymbol{g^T} = [1 \;\; 0 \;\; 0 \;\; 0 \dots \dots . .0] \dots \dots \dots . (3.36)$$

The aim is to find the weights $\boldsymbol{W^H}$ that satisfy all the former three constraints. Lagrange multipliers can be used here to solve this problem where the noise power which is given by $\boldsymbol{W^H}(w).\boldsymbol{S}_n(w).\boldsymbol{W}(w)$ must be minimized subject to the former three constraints that can be written in matrix form as $\boldsymbol{W^H}.\boldsymbol{C} = \boldsymbol{g^H}$. Consequently the Lagrangian is [12]:

$$\boldsymbol{J} = \boldsymbol{W^H}(w).\boldsymbol{S}_n(w).\boldsymbol{W}(w) + [\boldsymbol{W^H}.\boldsymbol{C} - \boldsymbol{g^H}]\boldsymbol{\lambda} + \boldsymbol{\lambda^H}[\boldsymbol{C^H}.\boldsymbol{W} - \boldsymbol{g}] \dots \dots \dots . (3.37)$$

The value of $\boldsymbol{W}$ that minimizes the above function needs to be found and this can be done by taking the complex gradiant of $\boldsymbol{J}$ with respect to $\boldsymbol{W}$ and setting it to zero [12]:

$$\boldsymbol{S}_n.\boldsymbol{W} + \boldsymbol{C\lambda} = \boldsymbol{0} \Rightarrow \boldsymbol{W} = -\boldsymbol{S}_n{}^{-1}\,\boldsymbol{C\lambda} \dots \dots \dots . (3.38)$$

$$\Rightarrow \boldsymbol{W^H}.\boldsymbol{C} = \boldsymbol{g^H} \Rightarrow -\boldsymbol{\lambda^H}\boldsymbol{C^H}\boldsymbol{S}_n{}^{-1}\,\boldsymbol{C} = \boldsymbol{g^H} \dots \dots \dots . (3.39)$$

Solving for λ^H and substituting in $\boldsymbol{W}$ gives [12]:

$$\boldsymbol{W^H = g^H[C^H S_n{}^{-1} C]^{-1} C^H S_n{}^{-1}} \ldots\ldots\ldots (3.40)$$

Assuming white noise this equation reduces to [12]: $\boldsymbol{W^H = g^H[C^H C]^{-1} C^H}$

4.4) Frost Beamformer:

Frost [11] proposed in 1972 an algorithm based on the constrained least mean squares CLMS to detect a signal coming from a desired direction and suppress noise and interference that arrive at other directions. It has been applied to solve problems in electromagnetics and it is based on minimizing the total power subject to a constraint [35]. It is classified as a broadband beamformer and can be modeled with a finite impulse response model as shown in Fig. 4.5:

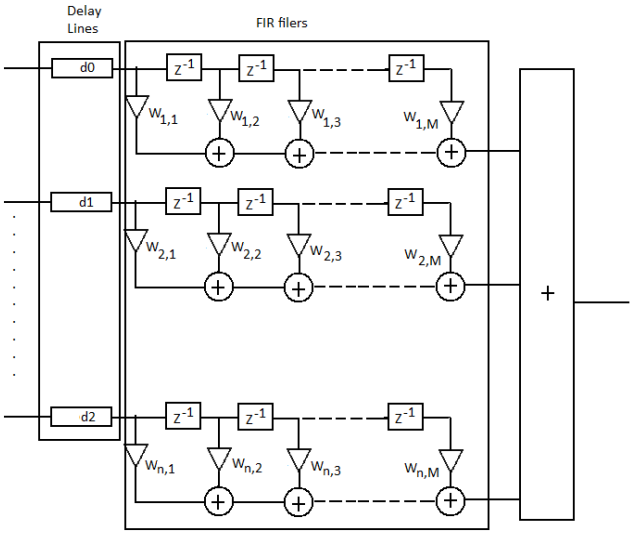

Figure 4.5. Frost beamformer

It consists of an array with K sensors and each sensor is followed by a transversal filter with J weights [35]. The weights are updated in order to minimize the CLMS of the output error where the impulse response of the whole system represents the constraint for the weights of all filters and must be equalized to unity [35]. To find the optimum

weights of this beamformer, let $X^T(k)$ be a vector of tap voltages at the k_{th}sample (because the voltages are sampled at the array taps) [11]:

$$\boldsymbol{X}^T(k) = \left[x_1(k\Delta), x_2(k\Delta), \dots\dots\dots, x_{KJ}(k\Delta)\right] \dots\dots\dots (3.41)$$

Where: T denotes a transpose. These tap voltages can be written as a sum of the signal in the desired direction and the noise signal that arrives from undesired directions [11]:

$$\boldsymbol{X}(k) = \boldsymbol{L}(k) + \boldsymbol{N}(k) \dots\dots\dots (3.42)$$

Where [11]:

$$L(k) = \begin{bmatrix} l(k\Delta) \\ \vdots \\ l(k\Delta) \end{bmatrix} \text{K Taps} \quad \begin{bmatrix} l(k\Delta - \tau) \\ \vdots \\ l(k\Delta - \tau) \end{bmatrix} \text{K Taps} \quad \begin{bmatrix} l(k\Delta - (J-1)\tau) \\ \vdots \\ l(k\Delta - (J-1)\tau) \end{bmatrix} \text{K Taps}$$

$$\boldsymbol{N}^T = [n_1(k\Delta), n_2(k\Delta), n_3(k\Delta), \dots\dots, n_{KJ}(k\Delta)]$$

The output of the beamformer is given as [11]:

$$\boldsymbol{y}(k) = \boldsymbol{W}^T\boldsymbol{X}(k) = \boldsymbol{X}^T(k)\boldsymbol{W} \dots\dots\dots (3.43), \qquad \boldsymbol{W}^T = \left[W_1, W_2, \dots\dots W_{KJ}\right]$$

The output signal power is [11]:

$$E[y^2(k)] = E[\boldsymbol{W}^T\boldsymbol{X}(k).\boldsymbol{X}^T(k)\boldsymbol{W}] = \boldsymbol{W}^T\boldsymbol{R}_{xx}\boldsymbol{W} \dots\dots\dots (3.44)$$

The aim is to make the impulse response represented by the weights equal to unity which can be expressed as [11]:

$$\boldsymbol{C_j}^T \boldsymbol{W} = \boldsymbol{f}_j \dots\dots\dots (3.45), \;\; j = 1,2,\dots,J$$

Where [11]:

$$\boldsymbol{C}_j = \begin{bmatrix} 0 \\ \vdots \\ 0 \\ 0 \\ \vdots \\ 0 \\ 1 \\ \vdots \\ 1 \\ 0 \\ \vdots \\ 0 \end{bmatrix} \begin{matrix} \} \text{K} \\ \} \text{K} \\ \} \text{K, } J_{th} \text{ group} \\ \} \text{K} \end{matrix}$$

Consequently, the constraint matrix can be defined as [11]:

$$\boldsymbol{C} = [\boldsymbol{C_1} \dots\dots \boldsymbol{C_j} \dots\dots \boldsymbol{C_J}] \quad \begin{matrix} \leftarrow \text{J} \rightarrow \\ \text{KJ} \end{matrix}$$

Also, $\boldsymbol{F}$ is defined as a J dimensional vector of weights of the desired direction [11]:

$$\boldsymbol{F} = \begin{bmatrix} f_1 \\ \vdots \\ f_j \\ \vdots \\ f_J \end{bmatrix}$$

Therefore; the constraints can be written in the following form [11]: $\boldsymbol{C^T W = F}$

The frequency response is fixed in the desired direction, therefore; minimizing the total output power in the undesired direction will minimize the noise power as well which may be expressed as follows [11]:

$$\text{Minimize } \boldsymbol{W^T R_{xx} W} \;\; ; \text{ Subject to } \boldsymbol{C^T W = F} \dots\dots\dots (3.46)$$

Where $\boldsymbol{R}_{xx}$is the signal autocorrelation function. Using Lagrange multipliers to solve this problem yields [11]:

$$\boldsymbol{\Lambda}(W) = \boldsymbol{W}^T \boldsymbol{R}_{xx} \boldsymbol{W} \quad + \lambda^T (\boldsymbol{C}^T \boldsymbol{W} - \boldsymbol{F}) \dots \dots \dots . (3.47)$$

Taking the gradient with respect to $\boldsymbol{W}$ [11]:

$$\boldsymbol{\nabla}_{\boldsymbol{W}} \boldsymbol{\Lambda}(W) = \boldsymbol{R}_{xx} \boldsymbol{W} \quad + \boldsymbol{C}\boldsymbol{\lambda} \dots \dots \dots . (3.48)$$

For optimality those two vector terms must be antiparallel and this can be accomplished by setting the sum to zero [11]:

$$\boldsymbol{\nabla}_{\boldsymbol{W}} \boldsymbol{\Lambda}(W) = \boldsymbol{R}_{xx} \boldsymbol{W} \quad + \boldsymbol{C}\boldsymbol{\lambda} = \boldsymbol{0} \dots \dots \dots . (3.49)$$

Consequently, the optimal weight vector is [11]:

$$\boldsymbol{W}_{\mathrm{OPT}} = -\boldsymbol{R}_{xx}^{-1} \boldsymbol{C}\boldsymbol{\lambda} \dots \dots \dots . (3.50)$$

$$\Rightarrow \boldsymbol{C}^T \boldsymbol{W}_{\mathrm{OPT}} = -\boldsymbol{C}^T \boldsymbol{R}_{xx}^{-1} \boldsymbol{C}\boldsymbol{\lambda} = \boldsymbol{F} \Rightarrow \boldsymbol{\lambda} = -[\boldsymbol{C}^T \boldsymbol{R}_{xx}^{-1} \boldsymbol{C}]^{-1} \boldsymbol{F} \dots \dots \dots . (3.51)$$

Therefore [11]:

$$\boldsymbol{W}_{\mathrm{OPT}} = \boldsymbol{R}_{xx}^{-1} \boldsymbol{C}[\boldsymbol{C}^T \boldsymbol{R}^{-1}{}_{xx} \boldsymbol{C}]^{-1} \boldsymbol{F} \dots \dots \dots . (3.52)$$

If $\boldsymbol{R}_{xx}$ is unknown and must be learned from the statistics of data using adaptive algorithm, then the next weight vector must take the form [11]:

$$\boldsymbol{W}(k+1) = \boldsymbol{W}(k) - \mu \boldsymbol{\nabla}_{\boldsymbol{W}} \boldsymbol{\Lambda}[\boldsymbol{W}(k)] = \boldsymbol{W}(k) - \mu[\boldsymbol{R}_{xx} \boldsymbol{W}(k) \quad + \boldsymbol{C}\boldsymbol{\lambda}(k)] \dots \dots \dots . (3.53)$$

Where $\boldsymbol{W}(k+1)$ must satisfy the same constraint [11]:

$$\boldsymbol{F} = \boldsymbol{C}^T \boldsymbol{W}(k+1) = \boldsymbol{C}^T \big[\boldsymbol{W}(k) - \mu[\boldsymbol{R}_{xx} \boldsymbol{W}(k) \quad + \boldsymbol{C}\boldsymbol{\lambda}(k)]\big] \dots \dots \dots . (3.54)$$

Solving for Lagrange multipliers $\boldsymbol{\lambda}(k)$ and substituting in the equation of $\boldsymbol{W}(k+1)$ gives [11]:

$$\boldsymbol{W}(k+1) = \boldsymbol{W}(k) - \mu[\boldsymbol{I} - \boldsymbol{C}(\boldsymbol{C^T C})^{-1}\boldsymbol{C^T}]\boldsymbol{R}_{xx}\boldsymbol{W}(k) + \boldsymbol{C}(\boldsymbol{C^T C})^{-1}[\boldsymbol{F} - \boldsymbol{C^T W}(k)]$$

$$\boldsymbol{W}(k+1) = \boldsymbol{P}[\boldsymbol{W}(k) - \mu\boldsymbol{R}_{xx}\boldsymbol{W}(k)] + \boldsymbol{U} \ldots\ldots\ldots (3.55)$$

Where:

$$\boldsymbol{P} = \boldsymbol{I} - \boldsymbol{C}(\boldsymbol{C^T C})^{-1}\boldsymbol{C^T}, \quad \boldsymbol{U} = \boldsymbol{C}(\boldsymbol{C^T C})^{-1}\boldsymbol{F}$$

Substituting: $\boldsymbol{R}_{xx} = \boldsymbol{X}(k).\boldsymbol{X^T}(k) \Rightarrow \boldsymbol{W}(k+1) = \boldsymbol{P}[\boldsymbol{W}(k) - \mu\boldsymbol{y}(k)\boldsymbol{X}(k)] + \boldsymbol{U}$ … (3.56)

4.5) Results and Findings:

In this section the results of this investigation are discussed and OriginLab software has been used to model some of the performance results in terms of deterministic mathematical functions. It has been assumed that all users are stationary in a multipath fading environment and the performance of each algorithm is evaluated under the same noise and interference conditions. First, the performance of the phase shift beamformer is investigated (equations 3.1-3.12). A phase shift beamformer is implemented at the transmitter and receiver sides of the intended user and two interfering sources are introduced from two different azimuth angles 80 and 20 degrees and the desired information signal arrives to the user from an azimuth angle of 45 degrees. The antenna array is a ULA and the antenna elements are separated by a half wavelength distance and the noise level is fixed while the interference level is varied. Different numbers of antenna elements are used and the results are shown in Fig. 4.6 below:

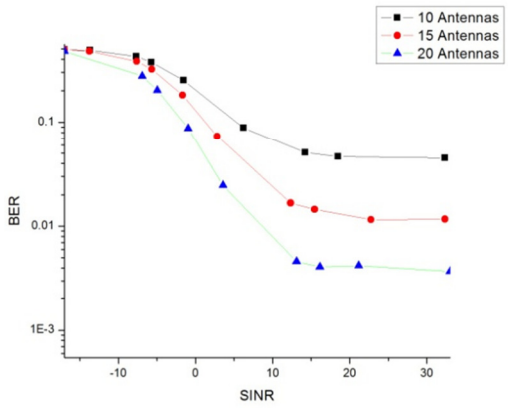

Figure 4.6 MIMO system performance using phase shift beamformer

It is clear that most of the performance improvement happens at low SINR (Signal to Noise plus Interference Ratio) and part of the negative SINR has been shown where the noise and interference power is higher than the signal power. As the number of antenna elements increases further improvement is achieved. In order to explain the effect of adding more elements on performance, the corresponding radiation pattern for the used number of elements is shown in Fig. 4.7 along with the time domain signals:

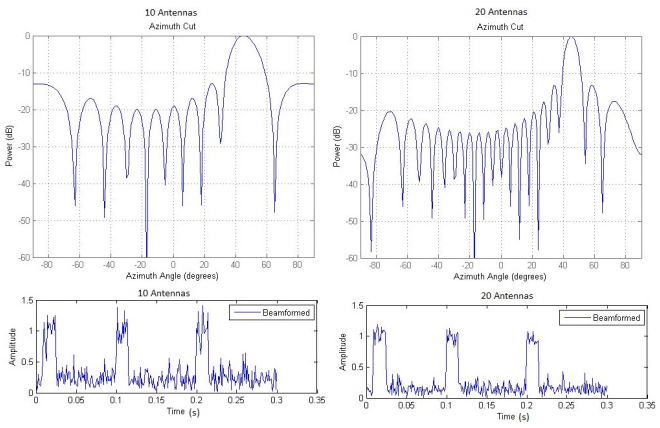

Figure 4.7 Phase shift beamformer approach

As the number of antenna elements increases, the beam directivity towards the desired direction which is at angle 45 becomes higher. This boots the signal power over noise and

interference and this is obvious in the time domain signals where reduction in noise and interference results in smoother pulses. However, as can be seen in the radiation pattern, the interferers at angles 20 and 80 could not be totally eliminated even when more antennas are used due to the existence of side lobs. Second, the MVDR beamformer has been implement (equations 3.13-3.26) at the receiver side while the transmitter employs phase shift beamformer (equations 3.1-3.5). It is simulated under the exact same conditions and assumptions of the Phase shift beamformer and here the results and findings are reported. Figure 4.8 shows the performance of the MVDR beamformer for different number of antenna elements along with time domain signals and a comparison with the phase shift beamformer is shown in the same figure:

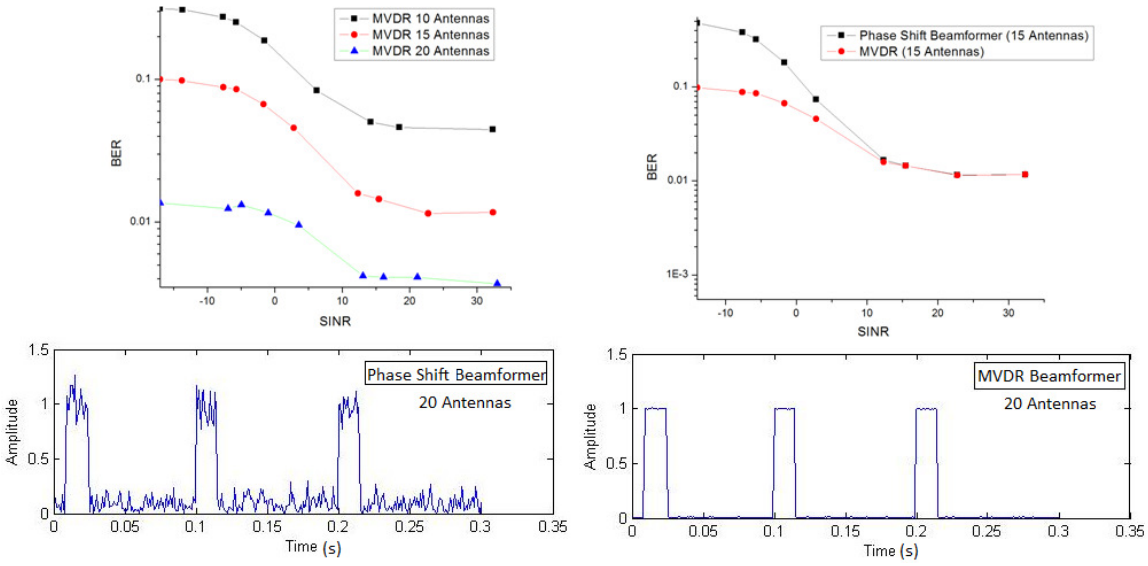

Figure. 4.8 Performance of MVDR and Phase shift beamformer

The performance of MVDR beamformer is different from that of phase shift at low SINR especially when the noise and interference powers are higher than the signal power and the time domain signals clarify this improvement. In MVDR the pulses are perfectly

recovered from noise and interference. To find the reason behind this difference the radiation patterns of both beamformers are illustrated in Fig. 4.9:

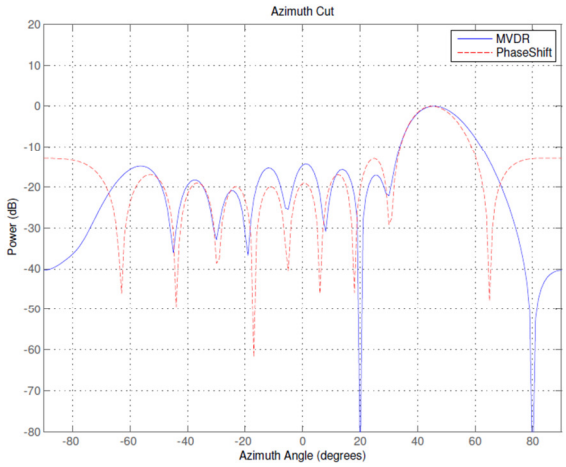

Figure 4.9 Radition pattern of MVDR and Phase shift beamformers

The radiation pattern helps explain the performance difference between the two beamformers. As can be seen on the figure, the MVDR beamformer shows higher interference suppression capability compared with the phase shift beamformer because it attenuates the signal in the direction of interferers at 20 and 80 degrees while the phase shift beamformer cannot provide the same suppression ability. However, at high SINR this difference in performance is eliminated as the phase shift beamformer can boost more power in the direction of the signal to achieve the same level of performance as the MVDR. It is not clear though which beamformer has higher noise mitigation as the radiation pattern does not show this information. Therefore, interferers have been eliminated and both beamformers were run in a noisy environment and the results are shown in Fig. 4.10:

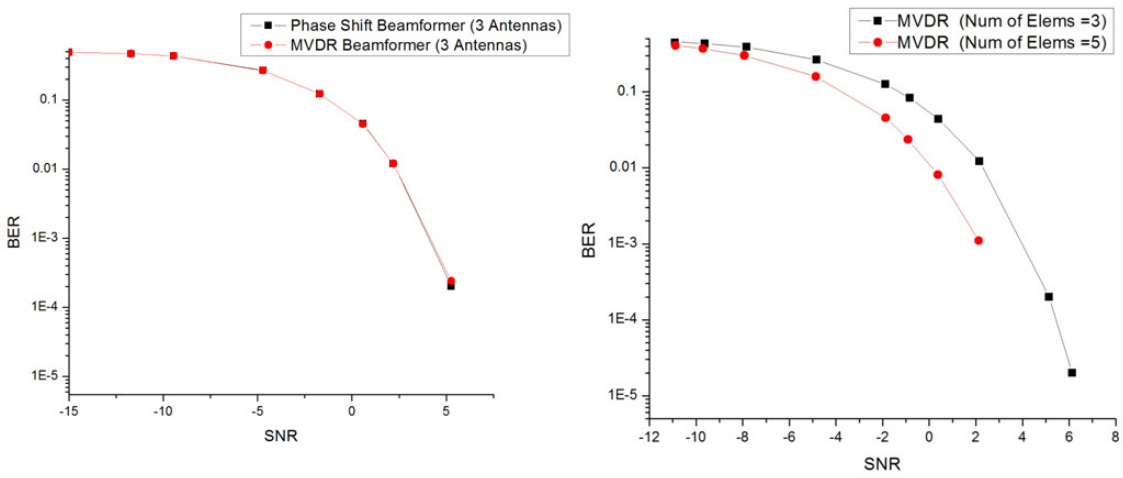

Figure 4.10. Performance of MVDR and Phase shift beamformer under noise only

The results in Fig. 4.10 are very important as they reveal a significant fact. Both beamformers show the exact same noise mitigation capability and this suggests that in a low interference environment and under moderate to high signal to interference ratios any of them can used, but if the interference floor becomes higher than the noise floor then MVDR becomes preferred as it offers better interference suppression. Further, as shown in the same figure; changing the number of elements in MVDR has a big impact on mitigating noise as well, because increasing the number of antenna elements from 3 to 5 results in better noise mitigation where the curve is shifted downwards when 5 elements are employed. Therefore, the number of antenna elements plays a major role not only in interference suppression but also in noise mitigation. The similarity in performance between the phase shift and MVDR beamformers in mitigating noise can be explained by fact that noise has the same effect on phase information in the phase shift beamformer and the steering vectors (which are phase shifts in the first place) in the MVDR beamformer. This makes those types of beamformers show a similar behavior concerning noise mitigation. In order to formulate a mathematical expression for the improved

performance in terms of the number of antenna elements for the sake of comparison with the diversity techniques (where performance was increased exponentially as more antennas were added to the receiver), OriginPro mathematical software has been used again for this purpose. It is assumed that no interference exists and only noise is present. Figure 4.11 shows the reported results:

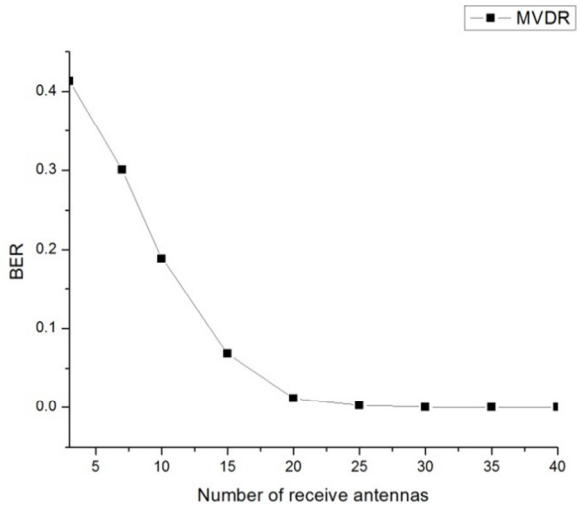

Figure 4.11. The effect of increasing the number of elements on BER (MVDR)

It has been found that this improvement shows the behavior of an exponential decay function which can be expressed as:

$$y = Ae^{-X/r} + y_0$$

Where: X represents the number of antenna elements and $A > 0, r > 0$, $y_0 < 0$ are constants. This result is interesting as the trend of performance improvement in beamforming systems is also an exponential but has a different degree at the exponent compared to the one found in the diversity systems. In figure 4.12 the corresponding

improvement in the SNR as the number of elements increases is shown to prove that the power becomes more concentrated with more antenna elements:

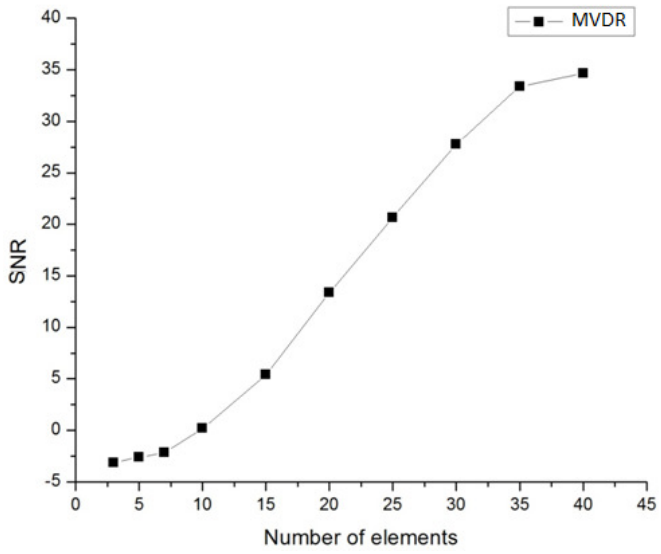

Figure 4.12. The effect of increasing the number of elements on SNR (MVDR)

This modeling showed that this curve follows an exponential growth function which is exactly the opposite of the former function and it can be expressed as:

$$y = Ae^{+X/r} + y_0$$

Where: X represents the number of elements and A, y_0, r are constants. This shows that the bit error rate decreases exponentially simultaneously as the SNR grows with the opposite exponent. Next, the performance of the LCMV beamformer (equations 3.27-3.40) is simulated under the same conditions of the previous beamformers where it has been implemented at the receiver and the desired signal arrives at an azimuth angle of 45 with two interfering sources at two azimuth angles of 20 and 80. The reported results are shown in Fig. 4.13 along with the performance of the MVDR beamformer for the sake of a fair comparison:

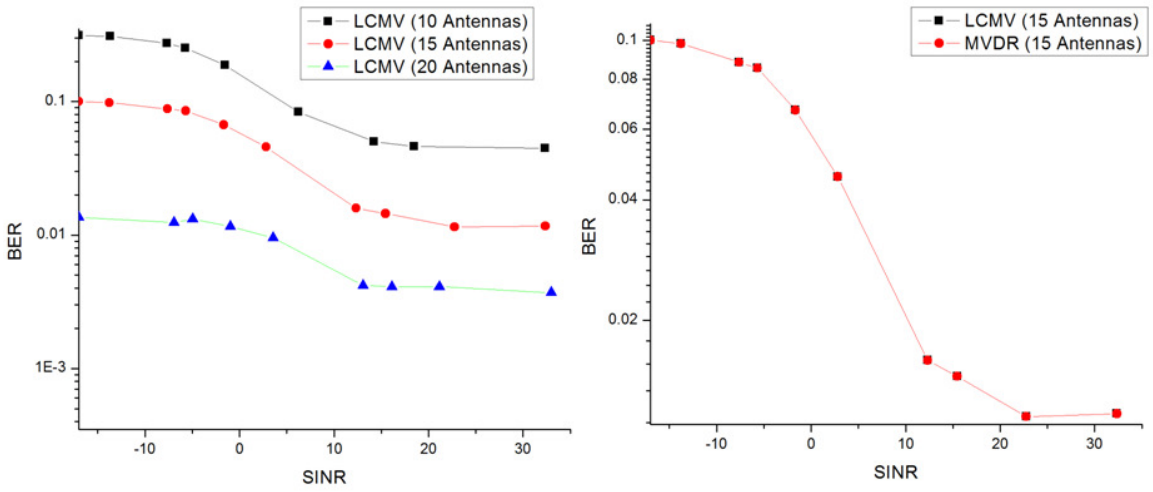

Figure 4.13 Performance of LCMV compared with MVDR

The results show exact same performance for both beamformers under the same conditions which clarifies that the imposed constraints of the LCMV beamformer have no effect at all if the assumed conditions do not change. Therefore, the LCMV beamformer has no privilege over the MVDR beamformer in such a situation. To double check this point both MVDR and LCMV beamformers are simulated again in two environments but under the same conditions for a fair comparison. In the first case only interference exists and no noise is present and in the second situation the exact opposite case in simulated where no interference exists but only noise is present and the reported results are shown in Fig. 4.14:

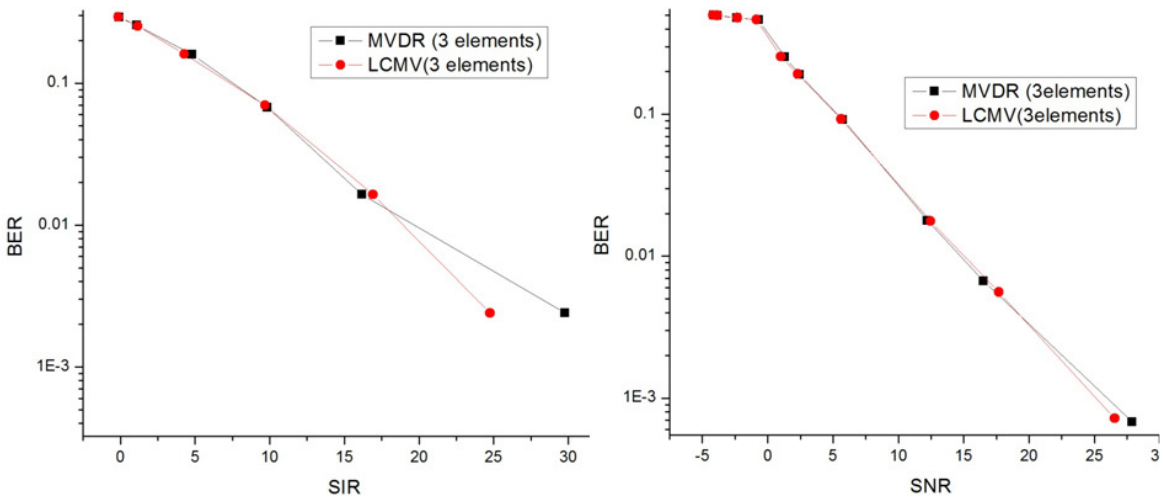

Figure 4.14. Comparison between MVDR and LCMV

The results show again that both LCMV and MVDR beamformers have the exact same performance under the same conditions for both noise and interference suppression where the left and right figures show the performance of interference suppression and noise mitigation respectively. In order to find the difference between the LCMV and MVDR beamformers, the expected direction of the desired signal has been changed for both beamformers to see if the constraints in the LCMV beamformer can give any difference in performance compared to the MVDR beamformer. For this purpose, the same simulation was run under the same conditions again with the presence of noise and interferece but in this case the direction of the desired signal has been changed to deviate from the expected direction by +5 degrees (equations 3.33) to become 50 instead of 45 (Direction of Arrival or DoA mismatch) and the results are shown in Fig. 4.15:

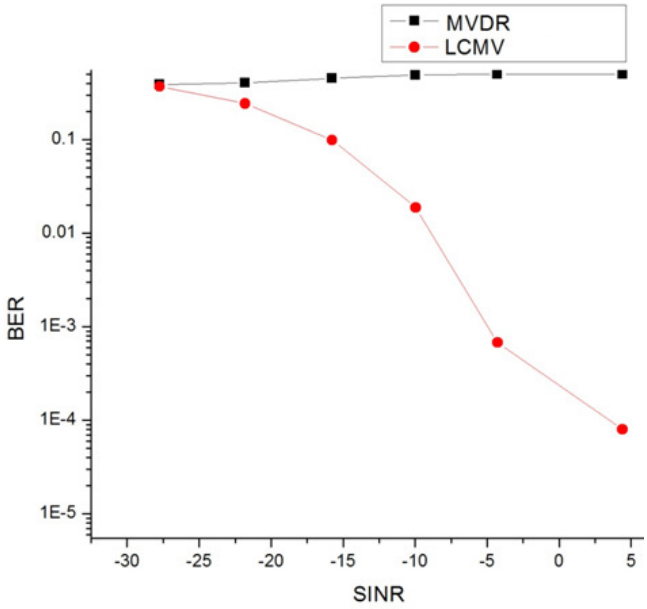

Figure 4.15 Comparison between MVDR and LCMV with DoA mismatch

The results show that the MVDR beamformer totally failed in achieving any acceptable performance when the signal did not arrive from the anticipated direction while the LCMV beamformer succeeded in extracting the desired signal. This clarifies the effect of the imposed constraints on performance when the working conditions change. To further visualize the effect, the radiation patterns of the both beamformers are shown in Fig 4.16:

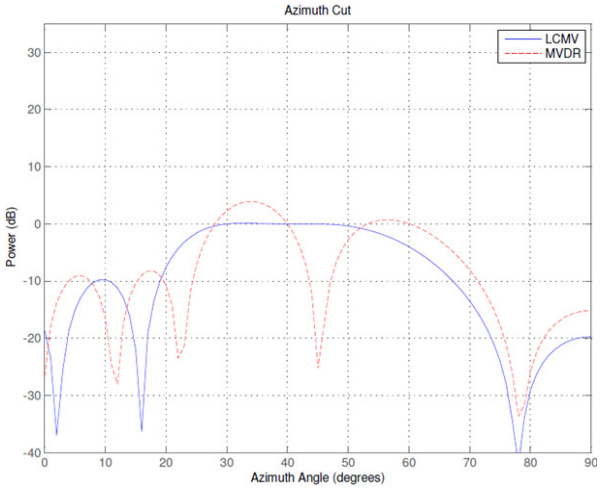

Figure 4.16 Radiation pattern of the MVDR and LCMV beamformers

It is obvious from the radiation pattern that the MVDR beamformer nulled the signal at 45 degrees because it has been treated as an interference signal while the LCMV beamformer succeeded in keeping track of the direction of the desired signal. Next the performance of Frost beamformer (equations 3.41-3.56) is investigated and compared with the rest of the algorithms. Frost beamformer has been simulated under the same conditions of the rest of the beamformers using 10 antennas in the absence of interference to find the noise mitigation ability of Frost compared to others and its performance is shown in Fig. 4.17:

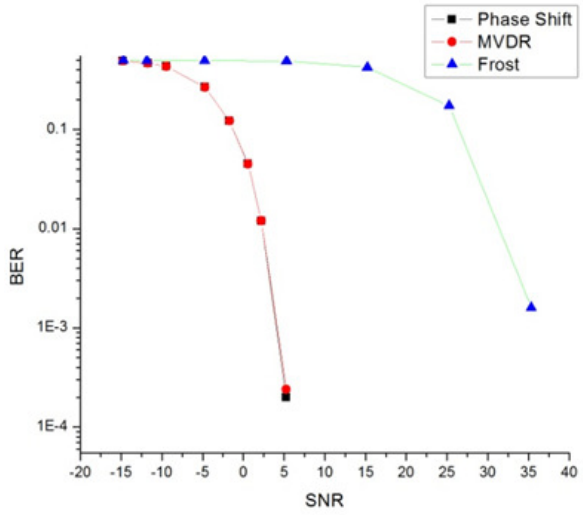

Figure 4.17 White noise mitigation of Frost

Frost appears to have the lowest performance among others. The reason behind this poor performance can be explained by the way it works which is based on minimizing the mean squared error of the whole signal which includes noise and the desired signal as well which consequently minimizes the desired signal power. This can be further explained by comparing the differences between the constraints that each beamformer imposes on its performance. Frost does not impose a distortionless constraint as in the MVDR beamformer (equations 3.18) but it minimizes the mean squared error (equation

3.44) which does not have perfect elimination of distortion as in the MVDR case. This limits its performance if the noise floor is higher than the interference floor as shown in Fig 4.18 below, while the rest of the investigated beamformers do not have this limitation because they have sufficient noise mitigation.

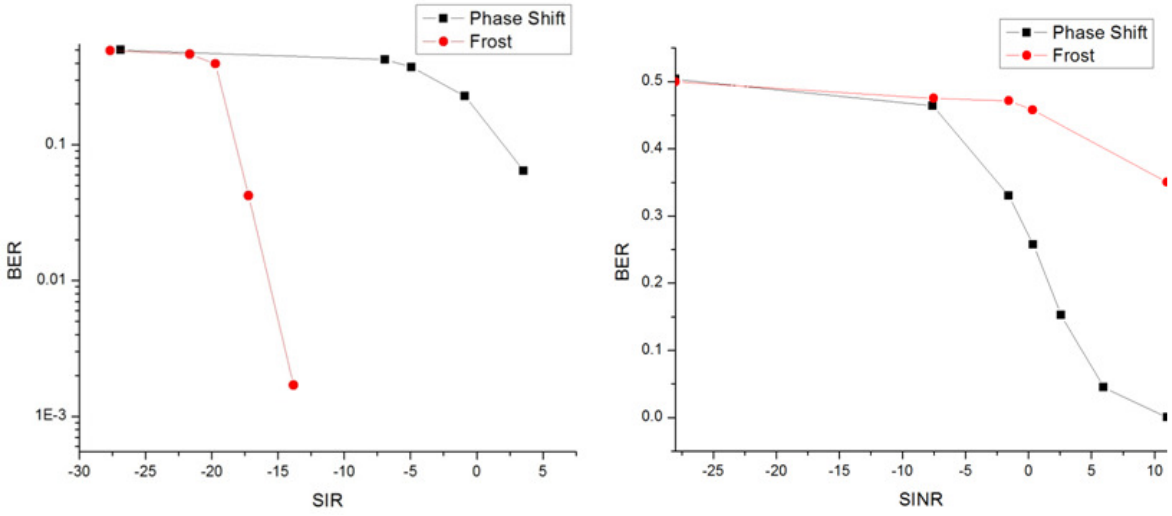

Figure 4.18 Frost Vs phase shift beamformers

The plots on the left and right show a comparison between the Frost and phase shift beamformers in a noise free and in a noise with interference environments respectively. The results show that Frost has better interference suppression capability than phase shift in the absence of noise but if high noise exists then the situation is revered where the phase shift outperforms Frost. In Fig. 4.19 a comparison between transmit diversity, receive diversity, spatial multiplexing and MVDR beamforming in the presence of noise and fading is shown where three antennas are employed in the receiver side for each scheme expect for the transmit diversity case where one antenna is used in the receiving station:

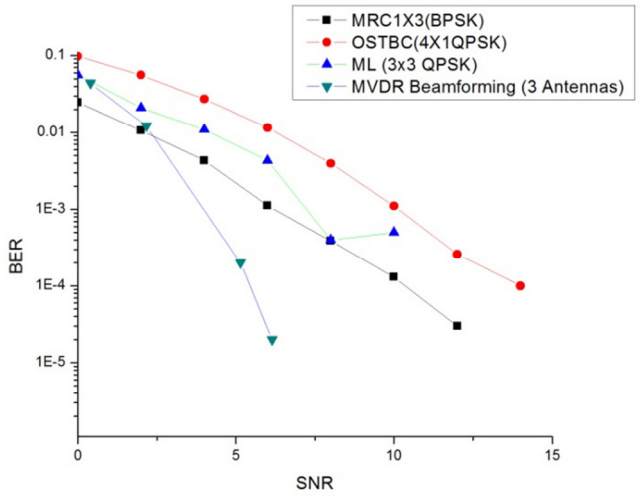

Figure 4.19 Comparison between all schemes

The most powerful method among all schemes is the MVDR beamforming where it outperforms the diversity schemes and this reveals that array gain is better than diversity gain therefore employing beamforming schemes in mobile and cellular systems shall result in high performance for all mobile users.

Chapter 5: Conclusions and Further Work

5.1) Conclusions:

In this thesis the performance of multiple antenna systems has been evaluated under similar conditions and key results have been reported. First, the transmit diversity scheme showed improved performance when more antennas were added to the transmitting station because this resulted in a higher diversity gain. However, receive diversity outperforms transmit diversity unless precoding which requires a perfect knowledge of channel state information is employed at the transmitter side. Spatial multiplexing techniques have a similar performance as the receive diversity techniques and increasing the diversity order in spatial multiplexing by using more antennas results in improved performance but still lower than the anticipated. This is due to the absence of space time coding in such schemes which shows the importance of space time coding in breaking the correlation between signal paths. Also, it was found that increasing the number of antennas at the receiver increases performance exponentially. The performance of single antenna receivers in multiuser MIMO highly depends on perfect knowledge of the channel state information where the regularized channel inversion showed the highest performance compared to others. This is because it decomposes the channel using the SVD method, while others use Cholesky decomposition which has higher roundoff errors that results in lower system performance. DPC outperforms THP although the later has higher bandwidth requirements and the reasons can be traced to manipulating the signal constellation which increases the error probability. In addition, the power saving characteristics in THP minimizes the signal power and results in lower signal to noise

ratios. Four different beamforming algorithms have implemented to simulate their performance in mobile communications and it has been found that phase shift, MVDR and LCMV beamformers share the same noise mitigation capabilities while they vary in suppressing interference. MVDR and LCMV have higher interference suppression than phase shift and LCMV outperforms MVDR in case of DoA mismatch. It has been found that increasing the number of antennas in MVDR beamformers improves performance exponentially as in space diversity systems but with a different order at the exponent. Frost beamformer has low noise suppression capability which limits its use in applications where the noise floor is higher than the interference floor. This has been confirmed when compared to the phase shift beamformer in such an environment where the phase shift outperformed Frost, but when noise was eliminated the opposite result was observed. Finally, when all the investigated schemes were compared; it was found that the MVDR and LCMV beamforming have superior performance can be considered as the optimal schemes for MIMO mobile communications.

5.2) Further Work:

There are a lot of unsolved problems in MIMO systems for both single user and multiuser scenarios. The single user MIMO systems were analyzed under the assumption of perfect knowledge of CSI. However, in real communication systems such knowledge may not be totally available and consequently other models that deal with such a situation remains an open problem for further investigation. On the other hand, the capacity of Gaussian broadcast channels is still an open problem as well [14] in addition to finding coding schemes for single antenna receivers that can achieve both high performance and power efficiency at once.

References:

[1] Yusuf Ozturk, Vaibhav Nagarnaik. (2010). Antenna diversity using single antenna in robot communication. *Digital Signal Processing*. Volume 20 (Issue 1), Pages 155–165.

[2] Siavash M. Alamouti. (1998). A Simple Transmit Diversity Technique for Wireless Communications. *IEEE JOURNAL ON SELECT AREAS IN COMMUNICATIONS*. VOL. 16, (NO. 8), Pages 1451-1458.

[3] A. Wittneben. (1991). Basestation modulation diversity for digital SIMULCAST. *Vehicular Technology Conference, 1991. Gateway to the Future Technology in Motion., 41st IEEE*, Pages 848 - 853.

[4] Wittneben, A. (1993). A new bandwidth efficient transmit antenna modulation diversity scheme for linear digital modulation. *ICC '93 Geneva. Technical Program, Conference Record, IEEE International Conference on Communications*. Volume 3, Pages 1630 - 1634.

[5] N. Seshadri, V. Tarokh and A.R. Calderbank. (1997). Space-Time Codes For Wireless Communication: Code Construction. *Vehicular Technology Conference, 1997, IEEE 47th*. Volume 2, Pages 637 - 641.

[6] Alamouti, S.M. ; Tarokh, Vahid ; Poon, P. (1998). Trellis-coded modulation and transmit diversity: design criteria and performance evaluation. *IEEE 1998 International Conference on Universal Personal Communications*. Volume 1, Pages 703 - 707.

[7] Caire, G.; Shamai, S. (2001). On achievable rates in a multi-antenna Gaussian broadcast channel. *IEEE International Symposium on Information Theory Proceedings*, Pages 147.

[8] Fischer, R.F.H. ;Windpassinger, C. ; Lampe, A. ; Huber, J.B. (2002). Tomlinson-

Harashima precoding in space-time transmission for low-rate backward channel. *International Zurich Seminar on Broadband Communications, Access, Transmission, Networking*, Pages 7-1 - 7-6.

[9] Christian B. Peel, Bertrand M. Hochwald, and A. Lee Swindlehurst. (2005). A Vector-Perturbation Technique for Near-Capacity Multiantenna Multiuser Communication—Part I: Channel Inversion and Regularization. *IEEE TRANSACTIONS ON COMMUNICATIONS*. VOL. 53 (NO. 1), Pages: 195-202.

[10] Lai-U Choi ; Murch, R.D. (2004). A transmit preprocessing technique for multiuser MIMO systems using a decomposition approach. *IEEE Transactions on Wireless Communications*. Volume: 3 (Issue: 1), Pages 20 - 24.

[11] OTIS LAMONT FROST. (1972). An Algorithm For Linearly Constrained Adaptive Array Processing. *PROCEEDINGS OF THE IEEE*. VOL. 60 (NO. 8), Pages 926-935.

[12] Harry L. Van Trees (2002). *Optimum Array Processing Part IV of Detection, Estimation, and Modulation Theory*. New York: John Wiley & Sons, Inc. Pages: 439-443,513-517,526-528.

[13] Arik D. Brown (2012). *Electronically Scanned Arrays*. Boca Raton: Taylor & Francis Group, LLC. Pages 2-6.

[14] Yong Soo Cho,Jaekwon Kim,Won Young Yang,Chung G. Kang (2010).*MIMO-OFDM WIRELESS COMMUNICATIONS WITH MATLAB*. Singapore: John Wiley & Sons (Asia) Pte Ltd. Pages: 71-75,278-279,281-289,294-297,319-322,327,328,373-382,395-416.

[15] Sajal K. Das (2010). *Mobile Handset Design*. Singapore: John Wiley & Sons Ltd. Page 66.

[16] Thiagarajan Viswanathan (2004). *Telecommunication Switching Systems and Networks*. New Delhi: Prentice-Hall of India Pvt.Ltd. Page 345.

[17] David Tse, Pramod Viswanath (2005). *Fundamentals of Wireless Communication*. New York: Cambridge University Press. Page 71.

[18] Pedersen, K.I; Mogensen, P.E. ; Fleury, B.H.. (2000). A Stochastic Model of the Temporal and Azimuthal Dispersion Seen at the Base Station in Outdoor Propagation Environments*, IEEE Transactions on Vehicular Technology*. Volume 49 (Issue 2), Pages 437 - 447.

[19] Kyōhei Fujimoto (2008). *Mobile Antenna Systems Handbook*. Norwood: ARTECH HOUSE, INC. Page 247.

[20] Prof. Lajos Hanzo, Dr. Yosef (Jos) Akhtman and Dr. Li Wang,Dr. Ming Jiang (2011). *MIMO-OFDM for LTE, Wi-Fi and WiMAX*. UK: John Wiley & Sons Ltd. Pages: 63-65.

[21] Love, D.J; Heath, R.W. (2005). Limited feedback unitary precoding for orthogonal space-time block codes*, IEEE Transactions on Signal Processing*. Volume 53 (Issue 1), Pages 64 - 73.

[22] Hochwald, B.M. ; Marzetta, T.L. ; Richardson, T.J. ; Sweldens, W. (2000). Systematic design of unitary space-time constellations. *IEEE Transactions on Information Theory*. Volume 46 (Issue: 6), Pages: 1962 - 1973.

[23] Tzi-Dar Chiueh, Pei-Yun Tsai, I-Wei Lai (2012). *Baseband Receiver Design for Wireless MIMO-OFDM Communications*. 2nd ed. Singapore: John Wiley & Sons Singapore Pte. Ltd. Pages 209-211.

[24] Waters, Deric W (2005). *Signal detection strategies and algorithms for multiple-*

input multiple-output channels (Doctoral dissertation). Ann Arbor: ProQuest/UMI. (Publication No. 3248792).

[25] Chaiman Lim ; Taesang Yoo ; Clerckx, B. ; Byungju Lee. (2013). Recent trend of multiuser MIMO in LTE-advanced. *IEEE Communications Magazine*. Volume: 51 (Issue: 3), Pages: 127 - 135.

[26] A. B. Gershman, N. D. Sidiropoulos (2005). *Space-Time Processing for MIMO Communications*. England: John Wiley & Sons Ltd. Pages: 83,84,217-219.

[27] Zhili Sun (2005). *Satellite Networking: Principles and Protocols*. England: Wiley. page 36.

[28] Vahid Dehdari, Clayton V. Deutsch. (2012). Applications of Randomized Methods for Decomposing and Simulating from Large Covariance Matrices. *Quantitative Geology and Geostatistics*. Volume 17, pp 15-26.

[29] Danial Ehyaie. *Novel Approaches to the Design of Phased Array Antennas* (Doctoral dissertation). University of Michigan, Ann Arbor: ProQuest/UMI, 2011. (Publication No. 3492769).

[30] Winters, J.H. (1998). Smart antennas for wireless systems. *IEEE Personal Communications*. Volume: 5 (Issue: 1), Pages 23 - 27.

[31] RONALD A. MUCCI. (1984). A Comparison of Efficient Beamforming Algorithms. *IEEE TRANSACTIONS ON ACOUSTICS, SPEECH, AND SIGNAL PROCESSING*. VOL. ASSP-32 (NO. 3), Pages: 548-558.

[32] Yikun Yu,Peter G.M. Baltus,Arthur H.M. van Roermund (2011).*Integrated 60GHz RF Beamforming in CMOS*. New York: Springer. Pages 22-28.

[33] David Havelock, Sonoko Kuwano, Michael Vorländer (2008). *Handbook of Signal*

Processing in Acoustics. New York: Springer. Page 698

[34] *Lagrange multiplier.* Available: http://en.wikipedia.org/wiki/Lagrange_multiplier. Last accessed 20th Sep 2013.

[35] Miroslav ˇ STRUPL, Pavel SOVKA. (2003). Analysis and Simulation of Frost's Beamformer. *RADIOENGINEERING*. Vol. 12 (NO. 2), Pages 1-9.